Am J Cancer Res 2020;10(5):1608-1629
www.ajcr.us /ISSN:2156-6976/ajcr0109672

Original Article

MLL5α activates AR/NDRG1 signaling to suppress prostate cancer progression

Yongjun Quan[1,2], Yun Cui[1], Wasilijiang Wahafu[1], Yuexin Liu[2], Hao Ping[2], Xiaodong Zhang[1]

[1]*Department of Urology, Beijing Chaoyang Hospital, Capital Medical University, Beijing 100020, China;*
[2]*Department of Urology, Beijing Tongren Hospital, Capital Medical University, Beijing 100730, China*

Received February 22, 2020; Accepted April 13, 2020; Epub May 1, 2020; Published May 15, 2020

Abstract: Prostate cancer (PCa) is one of the most prevalent malignancies in men. However, the molecular mechanism controlling the transformation of androgen-dependent PCa (ADPC) to castration-resistant PCa (CRPC) is largely unknown. Androgen receptor (AR) signaling has been reported to play a key role in this process; thus, searching for the novel AR co-activator is important for identifying the mechanism underlying PCa progression. In this study, we focused on the function of mixed lineage leukemia-5α (MLL5α), an epigenetic regulator that exhibits aberrant expression in PCa. MLL5α was the primary expressed form of MLL5 protein in PCa cells and it significantly suppressed proliferation, invasion, and migration in PCa cell lines. Upon stimulation with dihydrotestosterone (DHT), knockdown of MLL5α significantly suppressed N-myc downstream regulated gene 1 (NDRG1) and Kallikrein-related peptidase 3 (KLK3) expression. MLL5α directly bound with AR on the androgen response elements (AREs) and recruited H3K4me3 to the promoters of NDRG1 and KLK3. Downregulation of NDRG1 partially restored the cell invasion and migration suppressed by MLL5α. As evaluated by the proliferation of PCa cells, overexpression of MLL5α synergistically promoted sensitivity to enzalutamide (ENZ) treatment. In PCa patients, MLL5α expression was lower in the high Gleason score (GS) (GS > 7) group than in the low GS (GS < 7) group. In conclusion, suppression of AR/NDRG1 signaling via androgen deprivation therapy (ADT) may be a potential mechanism of CRPC progression. MLL5α significantly suppressed PCa progression by promoting AR/NDRG1 signaling, indicating that regulating MLL5α expression may be a potential treatment approach for patients with advanced PCa.

Keywords: Prostate cancer, MLL5α, AR, NDRG1, histone methylation, enzalutamide

Introduction

Prostate cancer (PCa) is one of the most prevalent malignancies and is a major cause of cancer-specific death in men [1]. PCa is primarily treated with castration therapy when it is in the androgen-sensitive stage. However, after a period of progression, the cancer transforms to a castration-resistant stage and ultimately metastasizes to bones, lungs, and other organs, which is the main cause of cancer-specific death in PCa patients.

The molecular mechanism controlling the transformation of androgen-dependent PCa (ADPC) to castration-resistant PCa (CRPC) is unclear. The most well-accepted theory is that androgen receptor (AR) signaling plays a crucial role in PCa progression. However, a far smaller body of convincing evidence indicates whether activation or repression of AR transcriptional activity occurs during the transformation of ADPC to CRPC. One review summarized the molecular mechanisms and proposed that AR functional amplification is the main reason for CRPC progression [2]. However, other recent studies advocated that androgen insensitivity in CRPC is caused by repression of AR transcription [3] and that metastasis of PCa also associated with androgen deprivation therapy (ADT) [4]. Neoadjuvant hormone therapy in CRPC significantly decreased the AR signature compared with that in untreated PCa [5], implying that decreasing AR function by castration may induce tumor progression. Studies have revealed that PCa tissues have lower AR expression than normal prostate tissues and benign hyperplastic tissues and that malignant PCa tissues also exhibit lower AR expression than high-

ly differentiated cancers [6-11]. Additionally, decreased AR expression led to poor prognosis and induced neuroendocrine differentiation in CRPC patients [9, 12-15].

Histones are components of nucleosome particles that form octamers, with approximately 147 base pairs (bp) of DNA wrapped around each octamer [16]. Chromatin structure is post-translationally regulated through histone modification at unique sites [17]. One of the common modifications is histone methylation. Methylation modifications of histone lysine (K) residues are divided into three types (KMe1, KMe2, and KMe3), and the epigenetic markers include histone 3 lysine 4 (H3K4), H3K9, H3K27, H3K36, and H3K79 [18, 19]. H3K4, H3K36 and H3K79 methylation induce target gene activation, and H3K9, H3K27, and H4K20 repress gene transcription [20].

Human mixed lineage leukemia-5 (MLL5), also called lysine methyltransferase 2E (KMT2E), belongs to the MLL family. As it is a methyltransferase, most studies have suggested that MLL5 participates in H3K4 methylation. However, there is strong controversy surrounding whether it intrinsically or indirectly regulates histone lysine methyltransferase (HKMT) activity [21-27]. The full-length MLL5 sequence contains 1858 amino acid residues (aa), and the smaller isoform MLL5α contains 609 aa [21, 23, 24]. MLL5α also contains a single plant homeodomain (PHD) zinc finger and a Su (var) 3-9, Enhancer of zeste, and Trithorax (SET) domain and thus may have the same function as H3K4 methyltransferases [22, 24]. The MLL5 chromatin profile suggests that full-length MLL5 targets only 60% of H3K4me3-containing promoters; the remaining promoters may be targeted by MLL5α [23]. The expression of MLL5α is also reported to be much higher than that of full-length MLL5 in undifferentiated HL60 cells and in human tissues [24]. We performed immunoblot analysis with an antibody specific for the amino terminal of MLL5 in PCa cell lines and found strong expression of MLL5α but negligible expression of full-length MLL5. Therefore, we assumed that MLL5α may be dominant over MLL5 in mediating epigenetic regulation via histone modification.

N-myc downstream regulated gene 1 (NDRG1), a well-known iron-regulated metastasis suppressor, has anti-metastatic functions in several cancers, including PCa [28-32]. AR binds to the promoter of NDRG1 and controls its transcriptional activity [33, 34]. However, the mechanism of AR-induced NDRG1 transcriptional activity is unclear.

In this study, we found that repression of AR/NDRG1 signaling through ADT may be a potential mechanism through which PCa progresses to CRPC. MLL5α significantly promoted AR/NDRG1 signaling by binding with AR and recruiting H3K4me3 to androgen response elements (AREs). Overexpression of MLL5α in PCa cells significantly suppressed PCa progression and promoted sensitivity to enzalutamide (ENZ) treatment.

Materials and methods

Cell culture

LNCaP, C4-2, 22RV1, PC3 and 293T cell lines were purchased from the American Type Culture Collection (Rockville, MD, USA). LNCaP, C4-2b, C4-2, 22RV1, and PC3 cells were cultured in RPMI-1640 medium supplemented with 10% fetal bovine serum (FBS) (HyClone, South Logan, UT, USA) and 1% antibiotic-antimycotic (AA) (Gibco, Grand Island, NY, USA). 293T cells were cultured in DMEM supplemented with 10% FBS and 1% AA. All cells were cultured at 37°C and 5% CO_2 in a humidified atmosphere.

Gene regulation in PCa cell lines

Lentiviruses harboring 3 × Flag-tagged MLL5α vectors were generated by GENECHEM (Shanghai, China). The pSGLV vector containing MLL5α short hairpin RNA (shRNA) or control shRNA (sh-NC) was constructed by Sangon Biotech (Shanghai, China). Lentiviruses were packaged via co-transfection of pSGLV (sh-MLL5α or sh-NC), pMD2.G, and psPAX2 into 293T cells with Lipofectamine 3000 (Invitrogen, Carlsbad, CA, USA) according to the manufacturer's instructions. After 10 hours (h) of co-transfection, the medium was changed, and culture was continued for 48 h before the lentivirus was harvested. Related cell lines were subjected to lentiviral transduction with 5 μg/ml polybrene for 24 h, and the medium was then changed. After 72 h, cells were selected using 1 μg/ml puromycin.

To transiently knock down NDRG1 expression in C4-2 and PC3 cells, NDRG1-specific small interfering RNA (siRNA) (GenePharma, Shanghai, China) was transfected into these cells with Lipofectamine 3000. The related sequences are shown in Supplementary Table 1.

Cell viability assay

A total of 2 × 10^3 cells were seeded in 96-well culture dishes and cultured for 48-96 h. Medium containing 10% Cell Counting Kit-8 (CCK-8) (MedChem Express (MCE), Monmouth Junction, NJ, USA) solution was then added and incubated for 1 h at 37°C. The absorbance of each well at 450 nm was measured in a microplate reader (Thermo Fisher Scientific Varioskan Flash, Waltham, MA, USA).

Colony formation assay

LNCaP cell lines (3 × 10^3 cells) and C4-2, 22RV, and PC3 cell lines (2 × 10^3 cells) were seeded in 6-well plates and cultured for 15 days to allow colony formation. Cells were fixed with 10% neutral buffered formalin solution and stained with 0.01% crystal violet solution (Beyotime, Shanghai, China). The number of colonies was counted after full decolorization.

Transwell assay

A Transwell assay was performed with Transwell chambers (Corning, NY, USA) to evaluate cell invasion. Matrigel (Cat# 356234, BD Biosciences, San Jose, CA, USA) was mixed 1:8 with pre-cooled RPMI medium (serum-free), and 50 μl was added to each upper chamber and incubated at 37°C for 2 h. Then, the supernatant in the upper chamber was removed, and 5 × 10^4 cells were added to serum-free medium. Five hundred microliters of RPMI medium supplemented with 20% FBS was placed into the lower chambers as a chemoattractant. Cells were incubated for 48 h, and cells on the upper surface of the Transwell membranes were removed. The membranes were fixed with 10% neutral buffered formalin solution and stained with 0.01% crystal violet solution (Beyotime). After full decolorization, the number of migrated cells was counted.

Wound healing assay

PCa cell lines (> 5 × 10^5) were seeded in 6-well plates at 90% confluence. Cells were scratched manually with a 200 μl pipette tip and cultured for 48 h. At 0 h, 24 h, and 48 h, cell movement was imaged via light microscopy. The mean migration distances were analyzed in ImageJ software (National Institutes of Health (NIH), Bethesda, USA).

Reverse transcription (RT) and quantitative real-time PCR (qPCR) analysis

Total RNA was isolated with TRIzol™ reagent (Invitrogen). To generate complementary DNA (cDNA), One-Step gDNA Removal and cDNA Synthesis SuperMix (TransGen Biotech, Beijing, China) with Anchored Oligo (dT) primers was used according to the protocol. qPCR was performed with Top Green qPCR SuperMix (TransGen Biotech) in an SDS 7500FAST Real-Time PCR system (Applied Biosystems, Foster City, CA, USA). GAPDH or 18S ribosomal RNA was used as the endogenous reference gene. The sequences of the relevant primers are shown in Supplementary Tables 2 and 3.

Western blot (WB) analysis

Cells or tissues were lysed in radio-immunoprecipitation assay (RIPA) buffer (Solarbio, Beijing, China) supplemented with 1:100 protease inhibitor cocktail (Sigma-Aldrich, St. Louis, MO, USA), 1:100 Phosphatase Inhibitor Cocktail 3 (Sigma-Aldrich), and 1:100 phenylmethylsulfonyl fluoride (PMSF) (Solarbio). The total protein concentration was quantified using a BCA Protein Assay Kit (KeyGen Biotech, Nanjing, China). A 1:4 volume of 5 × sodium dodecyl sulfate-polyacrylamide gel electrophoresis (SDS-PAGE) loading buffer (containing dithiothreitol (DTT)) (Solarbio) was added to the protein lysates and boiled at 100°C for 5 min. Then, proteins were separated on SDS-polyacrylamide gels and transferred to polyvinylidene difluoride (PVDF) membranes (Merck Millipore, Billerica, MA, USA). Membranes were blocked in 5% skim milk containing 1 × TBST (Solarbio). After 3 washes in TBST for 5 min each, membranes were incubated with primary antibodies overnight at 4°C in a swing bed. The next day, after 3 washes in TBST, membranes were incubated with secondary antibodies (diluted 1:5000) for 60 min. Immunoreactive bands were detected in a ChemiDoc™ XRS+ with Image Lab™ software (Bio-Rad, Hercules, CA, USA) using Chemiluminescent HRP Substrate (Merck Millipore). Information on the relevant

antibodies is shown in Supplementary Tables 4 and 5.

Co-immunoprecipitation (Co-IP) assay

LNCaP and C4-2 cells (1×10^7) were transduced with lentiviruses expressing 3 × Flag-tagged MLL5α. Cells were lysed with RIPA buffer and incubated with 5 μg of anti-AR (ab74272, Abcam, Cambridge, MA, USA) or anti-IgG (#2729, Cell Signaling Technology (CST), Danvers, MA, USA) antibodies for 6 h at 4°C with slow rotation. Then, protein A/G agarose beads (GE Healthcare, Little Chalfont, Buckinghamshire, UK) were added to the cell lysates and incubated for 2 h at 4°C with slow rotation. The immune complexes precipitated by the protein A/G agarose beads were eluted in denaturing SDS sample buffer, and WB analysis was performed with the anti-MLL5α, anti-Flag, and anti-AR antibody. Information on the relevant antibodies is shown in Supplementary Table 6.

Chromatin immunoprecipitation (ChIP) assay

ChIP assays were performed with an EZ-ChIP kit (Cat# 17-371, Merck Millipore) according to the instructions. The abundances of the immunoprecipitated genes were analyzed by PCR and qPCR. The primers for the NDRG1 promoter contained the ARE in the NDRG1 promoter at position -984, and the primers for the Kallikrein-related peptidase 3 (KLK3) promoter contained the AREs in the KLK3 promoter at positions -170 (ARE-I) and -394 (ARE-II). Detailed information on the ChIP assay-related oligonucleotide primers is shown in Supplementary Table 7.

Xenograft model establishment and treatment

An in vivo assay was carried out in accordance with the institutional ethical guidelines of Capital Medical University. Four-week-old male BALB/c athymic nude mice were provided by Beijing Vital River Laboratory Animal Technology Co., Ltd. (Beijing, China). C42-oeMLL5α or negative control (NC) cells (1×10^7) were mixed with 200 μl of phosphate-buffered saline (PBS) containing 30% Matrigel (BD Biosciences) and subcutaneously inoculated into the right axilla of mice. Twenty mice were intraperitoneally injected with 25 mg/kg/day ENZ (MCE) or dimethyl sulfoxide (DMSO) and randomly divided into four groups: oeNC-DMSO, oeMLL5α-DMSO, oeNC-ENZ, and oeMLL5α-ENZ. Tumor sizes were measured with calipers, and tumor volumes were calculated using the following formula: volume (mm^3) = (length × $width^2$) × 0.5. On the fiftieth day after cell inoculation, mice were euthanized and tumor tissues were taken out, and pathological analyses were performed.

Histological and immunohistochemical (IHC) analyses

Histological and IHC analyses were performed by Wuhan Servicebio Technology (Wuhan, China). Paraffin-embedded tissues were sectioned at 5 μm and subjected to antigen retrieval (or hematoxylin and eosin (HE) staining). Then, the sections were incubated with primary and secondary antibodies. To assess tumor proliferation, Ki-67 (#9449, CST) was assessed as described in a previous study [35]. Apoptosis was evaluated by staining with an anti-cleaved caspase-3 (C-Casp-3) antibody (#9661, CST) and terminal deoxynucleotidyl transferase (TdT) dUTP nick end labeling (TUNEL) (Roche, Basel, Switzerland). For statistical analysis, 6 fields at 400 × magnification were randomly selected, and the staining intensity score (1, weak; 2, moderate; 3, strong), the staining percentage score (0, ≤ 5% positive cells; 1, 6-25% positive cells; 2, 26-50% positive cells; 3, 51-75% positive cells; 4, ≥ 76% positive cells), and staining index (SI, staining intensity score × staining percentage score) were determined as described in previous studies [36, 37]. Data analyses were performed by another researcher who was blinded to each group.

Samples of PCa patients

All patients were recruited with approval from the Ethics Committee of Beijing Chaoyang Hospital Affiliated with Capital Medical University. Forty-five patients who were pathologically diagnosed with PCa (15 of Gleason score (GS) < 7, 15 of GS = 7, 15 of GS > 7) and underwent prostatectomy were enrolled between 2015 and 2018 in Beijing Chaoyang Hospital. Tissues were paraffin-embedded and stored in liquid nitrogen for use. All patients' pathological data were recorded, and patients were followed up through 2018.

Statistical analysis

In vitro experiments were conducted in triplicate or more for statistical significance. Continuous variables in two groups were analyzed

with a two-tailed Student's t-test or Mann-Whitney U test. For comparisons among 3 or more groups, one-way ANOVA followed by Tukey's or Dunnett's multiple comparisons post hoc tests were used. Categorical variables were analyzed with a Chi-square test. The results are shown as the means ± standard errors of the mean (SEMs), and $P < 0.05$ was considered statistically significant. Pearson correlation and linear regression analyses were performed to assess associations between genes, and a Pearson correlation coefficient (R) of > 0.3 and a *P* value of < 0.05 were considered to indicate a significant association between two genes. The Kaplan-Meier method was used for survival analysis, and a Cox regression model was used to evaluate the hazard ratio (HR). Statistical analyses were performed using SPSS software version 22 (IBM, Armonk, New York, USA), GraphPad Prism 7 software (GraphPad Software Inc., San Diego, CA, USA) or Microsoft Excel 2010 software.

Results

MLL5α affects the total level of H3K4 methylation in LNCaP cells and activates AR/NDRG1 signaling

The full-length and short isoforms of MLL5 were evaluated with an antibody specific for the amino terminus of MLL5 in different PCa (LNCaP, 22RV1, C4-2, and PC3) and prostate hyperplasia (BPH-1) cell lines. In WB analysis, MLL5α was expressed in all cell lines, but expression of full-length MLL5 was barely detected, even when the membrane was overexposed (**Figure 1Aa**). The mRNA levels of MLL5α in these cell lines were also detected. LNCaP, 22RV1, and C4-2 cells had relatively high expression of MLL5α, but BPH-1 and PC3 cells had low expression of MLL5α mRNA (**Figure 1Ab**).

To evaluate whether MLL5α regulated the total H3K4 methylation level, MLL5α expression was stably knocked down in LNCaP cells (sh-MLL5α; sh-NC cells were used as the negative control). Both cell lines were starved in serum-free medium for 24 h and were then treated with 20 nM dihydrotestosterone (DHT) or the same volume of ethyl alcohol (EtOH) for 24 h. As seen in the WB analysis, knockdown of MLL5α significantly reduced the global levels of H3K4me2 and H3K4me3 but did not significantly reduce the levels of H3K4me1 and H3K9me2/3 (**Figure 1B**).

Knockdown of MLL5α promoted the expression of neuroendocrine tumor markers (chromogranin A (CgA), synaptophysin (Syn), and neuron-specific enolase (NSE)), showing the potential transformation of ADPC to neuroendocrine PCa (NEPC) (**Figure 1C**). In parallel with the generation of LNCaP-sh-MLL5α/NC cells, MLL5α was stably overexpressed in C4-2 and PC3 cells (C42-oe-MLL5α/NC and PC3-oe-MLL5α/NC cells, respectively). The WB analysis results showed that knockdown of MLL5α in LNCaP cells suppressed the expression of NDRG1, AR, and E-cadherin but promoted the expression of N-cadherin. Overexpression of MLL5α in C4-2 and PC3 cells also promoted the expression of NDRG1 and AR (**Figure 1D**). We assessed other epithelial-mesenchymal transition (EMT) markers, which showed that knockdown of MLL5α in LNCaP cells tended to promote the expression of Slug, Snail, Vimentin, and ZEB1. Overexpression of MLL5α in C4-2 and PC3 cells also inhibited the expression of these markers (Supplementary Figure 1C).

MLL5α suppresses PCa cell proliferation, invasion, and migration

Cells with stable knockdown of MLL5α (LNCaP cells) or overexpression of MLL5α (22RV1 and C4-2 cells) were generated via lentiviral transduction. In the CCK-8 and colony formation assays, knockdown of MLL5α increased the proliferation of LNCaP cells, and overexpression of MLL5α reduced the proliferation of 22RV1 and C4-2 cells (**Figure 2A-D**). In the Transwell assay and wound healing assay, knockdown of MLL5α promoted the invasion of LNCaP cells (**Figure 2E**). In addition, overexpression of MLL5α significantly suppressed the invasion and migration of 22RV1 and C4-2 cells (**Figure 2F**, **2G**).

MLL5α directly binds with AR at AREs in NDRG1 and KLK3 to promote the expression of these genes

LNCaP and C4-2 cells were transduced with lentiviruses expressing 3 × Flag-tagged MLL5α (LNCaP-oe-MLL5α and C42-oe-MLL5α), and a Co-IP assay was performed. Immunoprecipitation was conducted with anti-AR and anti-IgG antibodies, and immunoblotting was performed with anti-MLL5α, anti-Flag, and anti-AR antibodies. Flag-tagged MLL5α precipitated with AR, showing the formation of an MLL5α-AR complex (**Figure 3A**).

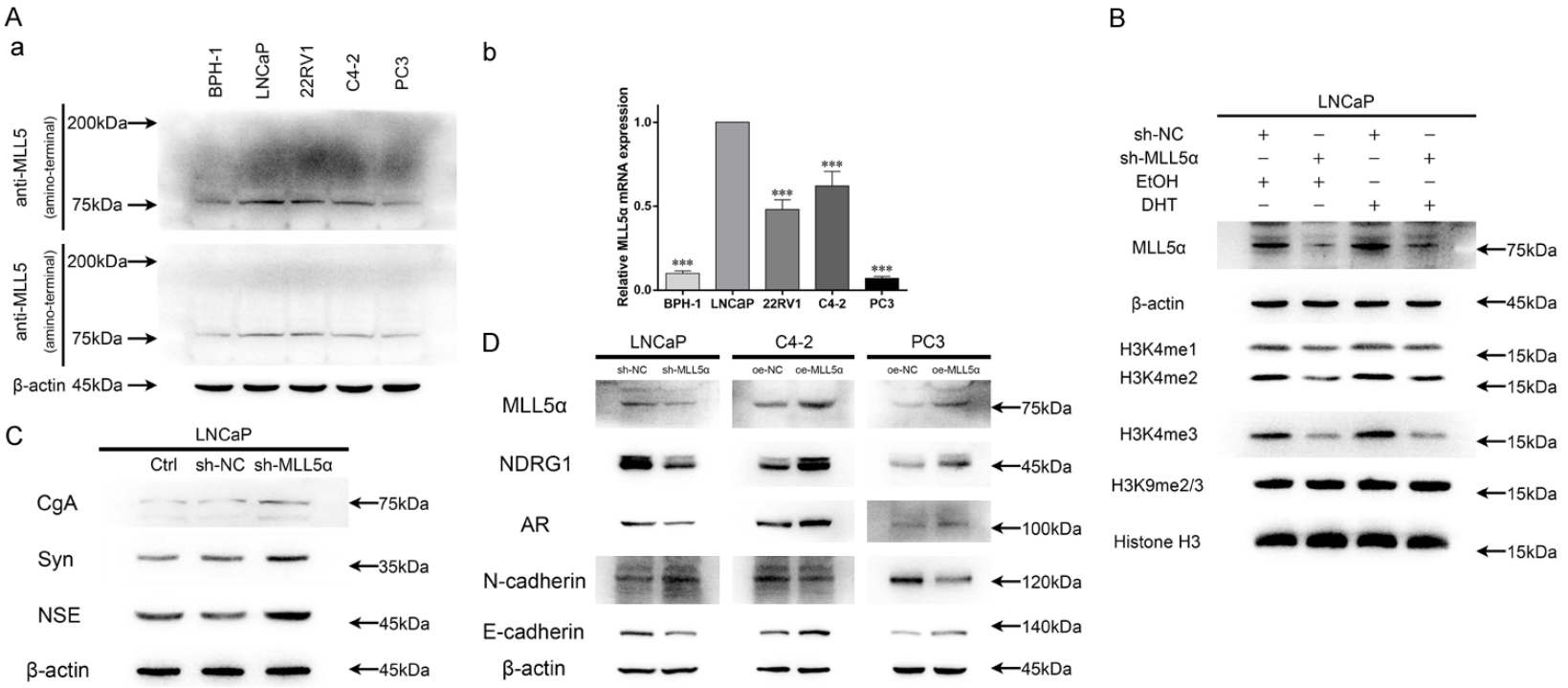

Figure 1. MLL5α affects the total level of H3K4 methylation in LNCaP cells and activates AR/NDRG1 signaling. A. The protein levels (a) of MLL5 and MLL5α were determined through WB analysis with an antibody specific for the amino terminus of MLL5. Relative mRNA levels (b) were assessed through qPCR analysis in BPH-1, LNCaP, 22RV1, C4-2, and PC3 cell lines (vs LNCaP). The results are presented as the means ± SEMs. ***P < 0.001. B. MLL5α expression was stably downregulated in LNCaP cells via lentiviral transduction (sh-MLL5α, with sh-NC as the negative control). Both cell lines were starved in serum-free medium for 24 h and were then treated with 20 nM DHT or the same volume of EtOH for 24 h. Protein levels were then assessed via WB analysis with histone methylation-related antibodies. C. WB was performed in LNCaP-shMLL5α/NC cells (Ctrl, parental LNCaP cells) with antibodies against neuroendocrine markers. D. The expression of MLL5α was downregulated in LNCaP cells (sh-NC and sh-MLL5α) and was upregulated in C4-2 and PC3 cells (oe-NC and oe-MLL5α). WB analysis was performed with AR/NDRG1 signaling-related antibodies.

To estimate MLL5α-regulated AR transcriptional activity, LNCaP-sh-MLL5α/NC cells were treated with 20 nM DHT or EtOH, and the expression levels of representative AR-responsive genes (ARGs) were evaluated via qPCR. After DHT treatment, knockdown of MLL5α in LNCaP cells significantly reduced the mRNA expression levels of prostate transmembrane protein androgen induced 1 (PMEPA1), NDRG1, and KLK3 ($P < 0.05$) (**Figure 3B**). To further elucidate the MLL5α-specific AREs in NDRG1 and KLK3, LNCaP-oe-MLL5α cells were treated with EtOH or DHT for 24 h and were then subjected to a ChIP assay. Cross-linked lysates were immunoprecipitated with anti-IgG or anti-Flag antibodies, and AREs in the NDRG1 and KLK3 promoters were detected via PCR and qPCR. 3 × Flag-tagged MLL5α significantly precipitated with the AREs of NDRG1 and KLK3; DHT treatment also stimulated these reactions (**Figure 3C**).

MLL5α induces AR and H3K4me3 recruitment to the AREs in NDRG1 and KLK3

Although MLL5α was shown to form a complex with AR and to directly bind with the AREs in NDRG1 and KLK3, the effect of MLL5α on the AR binding efficiency and whether MLL5α plays a role in histone methylation at binding sites were unclear. Therefore, LNCaP-sh-MLL5α/NC cells were treated with 20 nM DHT or EtOH, and ChIP assays were performed via immunoprecipitation with anti-H3K4me3, anti-AR, and anti-IgG antibodies. AREs in the NDRG1 and KLK3 promoters were detected via PCR and qPCR. As shown in the results, knockdown of MLL5α significantly reduced AR binding with the AREs in NDRG1 and KLK3 and decreased H3K4me3 recruitment to these AREs (**Figure 4A**). For further confirmation, MLL5α was stably overexpressed in C4-2 cells, and ChIP assays were performed with the same antibodies used for immunoprecipitation. Overexpression of MLL5α significantly induced both AR binding and H3K4me3 modification in the AREs of NDRG1 and KLK3 (**Figure 4B**). We concluded that MLL5α is necessary for AR binding with AREs and that it functions in histone methylation to influence AR transcriptional activity.

MLL5α suppresses PCa cell invasion and migration by activating AR/NDRG1 signaling

To assess the relationship of AR/NDRG1 signaling with MLL5α-induced cell proliferation, invasion, and migration, MLL5α was overexpressed in C4-2 and PC3 cells (C4-2/PC3-oe-MLL5α/NC) via lentiviral transduction, and NDRG1 expression was transiently inhibited through siRNA transfection (si-NDRG1/NC). Regulation of MLL5α and NDRG1 was verified via WB analysis and qPCR (Supplementary Figure 1D). In the CCK-8 assay, Transwell assay, and wound healing assay, inhibition of NDRG1 significantly restored the cell invasion and migration suppressed by MLL5α but did not restore proliferation (**Figure 5A-C**).

Overexpression of MLL5α promotes PCa cell sensitivity to ENZ treatment

C4-2/PC3-oe-MLL5α/NC cells were treated with 20 μM ENZ or the same volume of DMSO. Cell proliferation was assessed via CCK-8 and colony formation assays. MLL5α overexpression and ENZ treatment synergistically suppressed the proliferation of C4-2 and PC3 cells (**Figure 6A**, **6B**).

In the in vivo assay, xenograft mouse models were established using C42-oe-MLL5α/NC cells. Twenty mice were intraperitoneally injected with 25 mg/kg/day ENZ or the same volume of DMSO and were randomly divided into four groups: oeNC-DMSO, oeMLL5α-DMSO, oeNC-ENZ, and oeMLL5α-ENZ. On the fiftieth day after cell inoculation, mice were euthanized, and the tumors were completely removed (**Figure 6C**). Compared with other groups, the oe-MLL5α-ENZ group exhibited the lowest tumor volumes and weights (normalized to the oe-NC-DMSO group: 62.3% in the oeMLL5α-DMSO group, 50.9% in the oeNC-ENZ group, and 15.0% in the oeMLL5α-ENZ group) (**Figure 6D**).

Tumors were harvested and subjected to IHC analysis and HE staining (**Figure 6E**). The IHC staining percentage and staining index of the TUNEL positivity was significantly higher, and the levels of Ki-67 were significantly lower in the oeMLL5α-ENZ group than in the oeNC-DMSO group ($P < 0.05$). Although the levels of cleaved caspase-3 (C-Casp-3) were not significantly different, the oeMLL5α-ENZ group exhibited a trend towards an increase compared with the oeNC-DMSO group ($P = 0.1101$ for the staining percentage and $P = 0.6747$ for the staining index) (**Figure 6F**). These results showed that MLL5α overexpression and ENZ treatment synergistically promoted tumor apo-

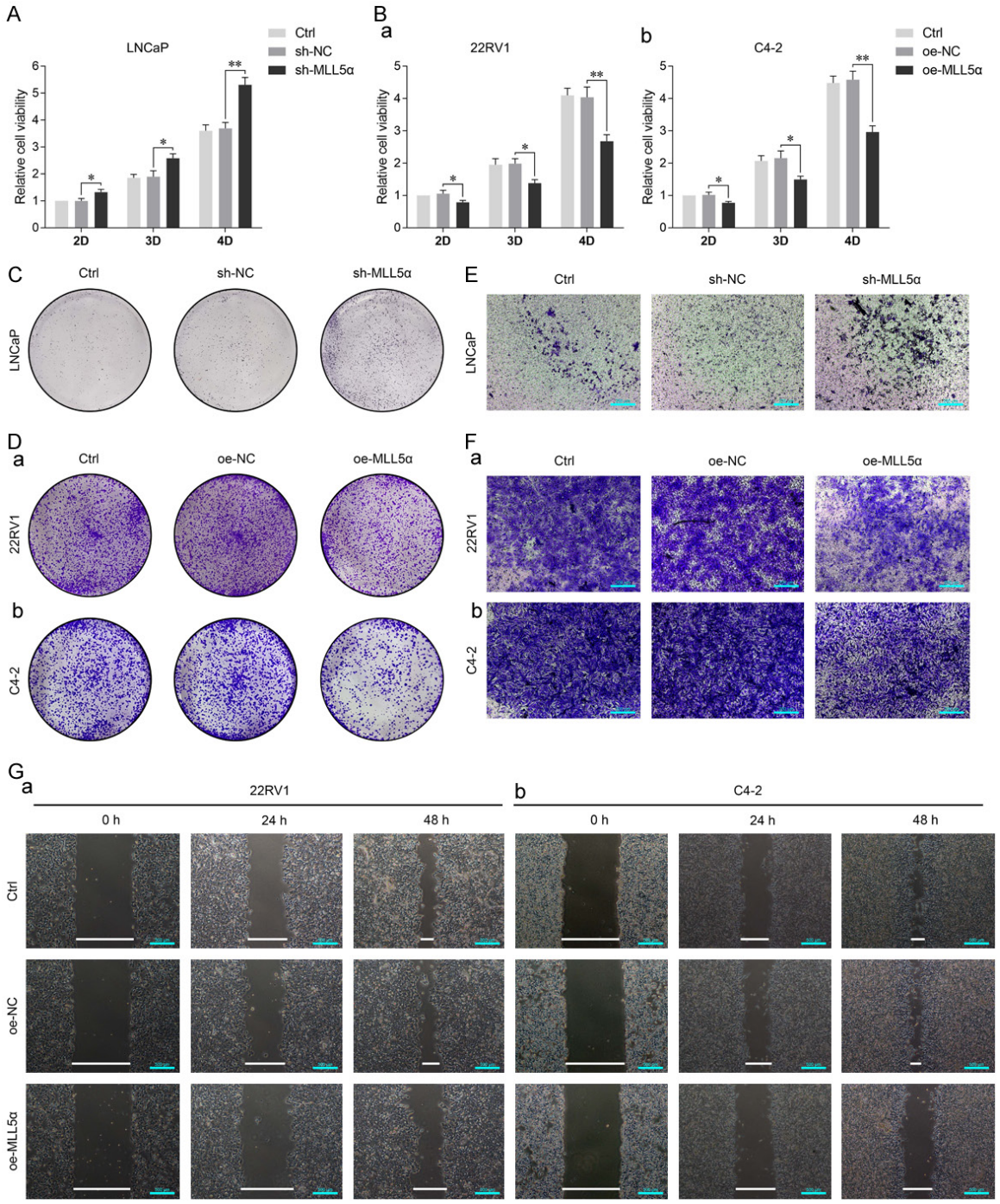

Figure 2. MLL5α suppresses PCa cell proliferation, invasion, and migration. The expression of MLL5α was downregulated in LNCaP cells (A, C, and E) (sh-MLL5α/NC and Ctrl cells) and was upregulated in 22RV1 (Ba, Da, Fa, and Ga) and C4-2 cells (Bb, Db, Fb, and Gb) (oe-MLL5α/NC and Ctrl cells). Then, we assessed cell proliferation, invasion, and migration by performing CCK-8 assays (A and B), colony formation assays (C and D), Transwell assays (E and F), and wound healing assays (G). The results are presented as the means ± SEMs. *P < 0.05 and **P < 0.01.

ptosis and inhibited tumor growth in the xenograft mouse model. In the HE staining images, the cells from the oeMLL5α-ENZ group exhibited empty nuclei and indistinct boundaries compared with those from the other groups.

Low expression of MLL5α is observed in advanced stages of PCa

A total of 45 PCa patients who underwent prostatectomy were enrolled at Beijing Chaoyang

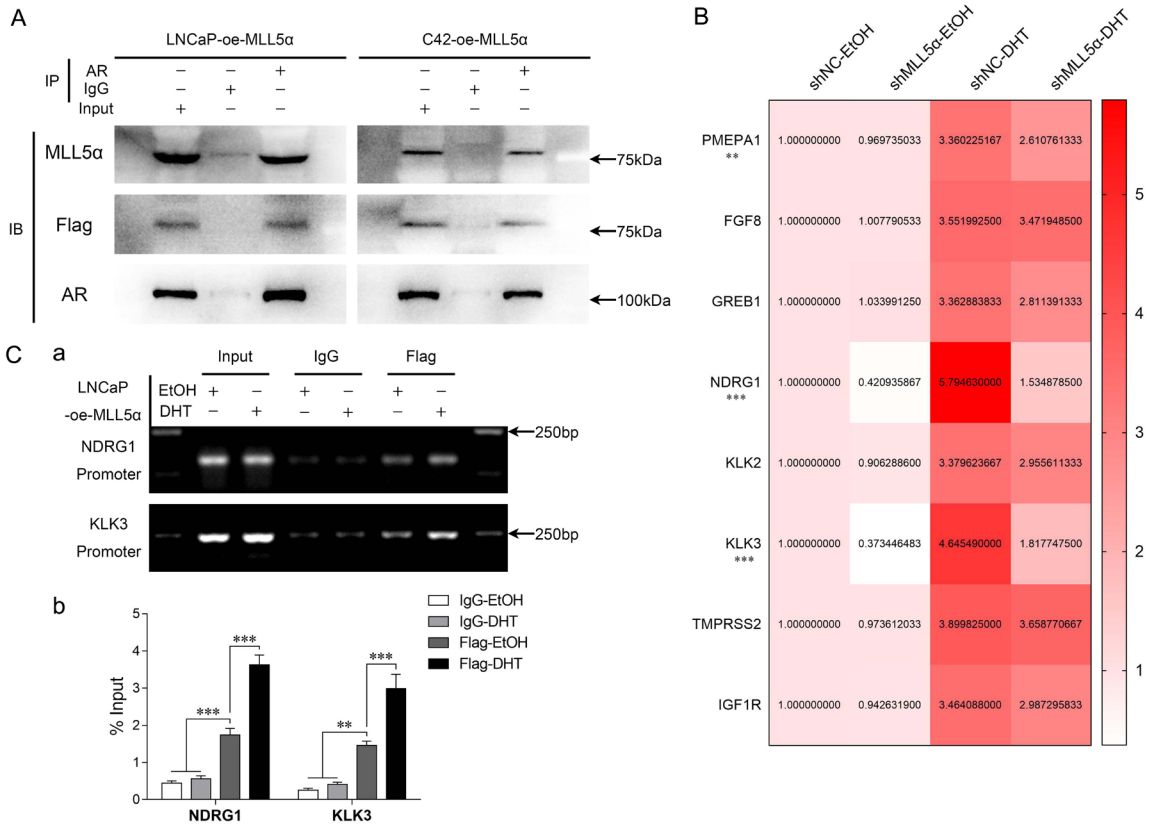

Figure 3. MLL5α directly binds with AR at the AREs in NDRG1 and KLK3 to promote the expression of these genes. (A) 3 × Flag-tagged MLL5α was overexpressed in LNCaP and C4-2 cells (LNCaP-oe-MLL5α and C42-oe-MLL5α, respectively), and a Co-IP assay was performed. Immunoprecipitation was conducted with anti-AR and anti-IgG antibodies, and immunoblotting was performed with anti-MLL5α, anti-Flag, and anti-AR antibodies (IP: immunoprecipitation; IB: immunoblotting). (B) LNCaP-sh-NC and LNCaP-sh-MLL5α cells were treated with 20 nM DHT or EtOH, and the mRNA levels of ARGs were evaluated via qPCR analysis. The relative expression levels of ARGs in LNCaP-sh-MLL5α and LNCaP-sh-NC were statistically analyzed (shNC-DHT vs shMLL5α-DHT). Results are presented as the means. **P < 0.01 and ***P < 0.001. (C) LNCaP-oe-MLL5α cells were treated with 20 nM DHT or EtOH and were then subjected to a ChIP assay through immunoprecipitation with anti-IgG or anti-Flag antibodies. The AREs of NDRG1 and KLK3 were detected via PCR (a) and qPCR (b) assays. The results are presented as the means ± SEMs. **P < 0.01 and ***P < 0.001.

Hospital. As shown in the clinical characteristics, the patients were divided into two groups according to the median MLL5α mRNA expression level (**Table 1**). Low expression of MLL5α was trended to higher GS (P = 0.083), higher clinical T stage (P = 0.031), and incidence rates of lymph node metastasis (P = 0.035). Although the incidence rates of distant metastasis (P = 0.619) and the TNM stage III-IV disease (P = 0.175) did not significantly differ between the groups, the percentages of stage M1 (low:high = 18.2%:8.7%) and TNM stage III-IV disease (low:high = 45.5%:26.1%) were higher in the group with low MLL5α expression.

Fifteen adjacent normal prostate tissues were randomly included as controls. Based on the different GSs, the PCa tissues were divided into 4 groups: normal tissue, GS ≤ 6, GS = 7, and GS ≥ 8. The IHC analysis results showed that both the percentage of MLL5α-positive cells and the MLL5α staining index were significantly reduced in the GS ≥ 8 group compared with the normal tissue and GS ≤ 6 groups (**Figure 7A**). Regarding the mRNA level of MLL5α, 80% of randomly selected PCa tissues exhibited downregulation compared with adjacent normal tissues, and the GS ≥ 8 group exhibited reduced MLL5α expression compared with the normal tissue and GS ≤ 6 groups (P < 0.05) (**Figure 7B**). The protein levels of MLL5α were assessed by WB analysis in 8 PCa tissues and associated adjacent normal tissues (P1-P8). These results showed that 75% of the patients (P3-P8) had lower expression of MLL5α in the PCa tissues than in the normal

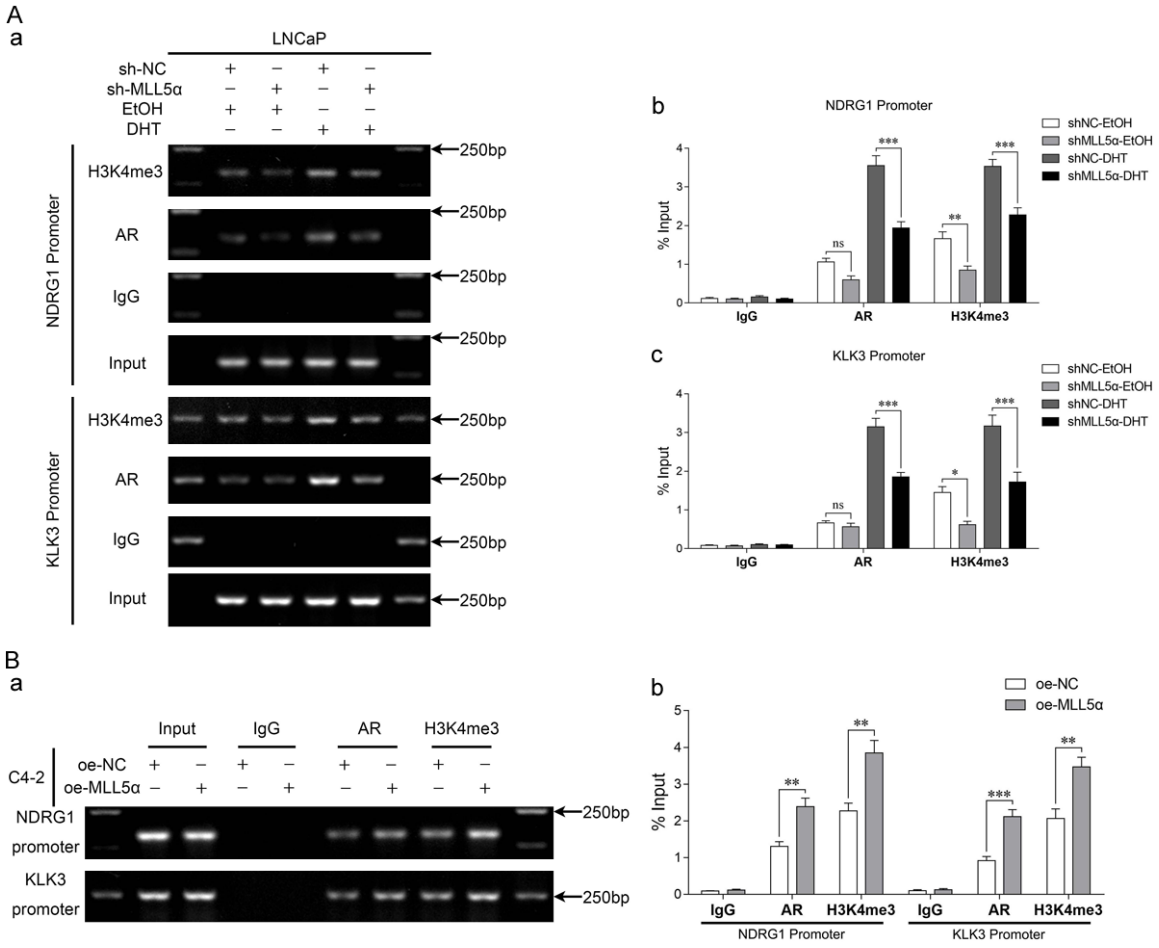

Figure 4. MLL5α induces AR and H3K4me3 recruitment to the AREs in NDRG1 and KLK3. (A) LNCaP-sh-MLL5α/NC cells were treated with 20 nM DHT or EtOH, and a ChIP assay was performed through immunoprecipitation with anti-H3K4me3, anti-AR, and anti-IgG antibodies. The AREs in the NDRG1 and KLK3 promoters were detected via PCR (a) and qPCR (b and c). The results are presented as the means ± SEMs. ns $P > 0.05$, *$P < 0.05$, **$P < 0.01$, and ***$P < 0.001$. (B) MLL5α was overexpressed in C4-2 cells (C42-oe-MLL5α, with C42-oe-NC as the negative control), and a ChIP assay was performed with the same antibodies noted in (A). PCR (a) and qPCR (b) were performed to assess the AREs in NDRG1 and KLK3. The results are presented as the means ± SEMs. **$P < 0.01$ and ***$P < 0.001$.

tissues (**Figure 7Ca**). According to the patients' pathological data, we also assessed 12 PCa patients with a low GS (GS < 7) and a high GS (GS > 7). MLL5α protein expression was lower in patients with a high GS (**Figure 7Cb**).

Low expression of MLL5 was associated with poor recurrence-free survival of PCa patients in the Taylor Prostate 3 database

Further evaluation of the effect of MLL5α on the prognosis of PCa patients was limited by the number of patients in this study. We obtained the Taylor Prostate 3 database and evaluated the relationships of MLL5, NDRG1, KLK3, and AR with survival. To reduce inaccurate reporter bias in Pearson correlation analysis and linear regression analysis, we selectively removed a few individual data points (< 15; the total number was 185) that were out of range (we mainly selected reported expression values of AR < 7, NDRG1 < 26, and KLK3 > 10 for analysis). The correlation analysis results indicated that the mRNA expression levels of MLL5, NDRG1, KLK3, and AR were positively correlated with each other ($R > 0.3$ and $P < 0.001$) (**Figure 8Aa-f**).

With the data on recurrence follow-up time and overall survival follow-up time provided in the Taylor Prostate 3 database, we performed

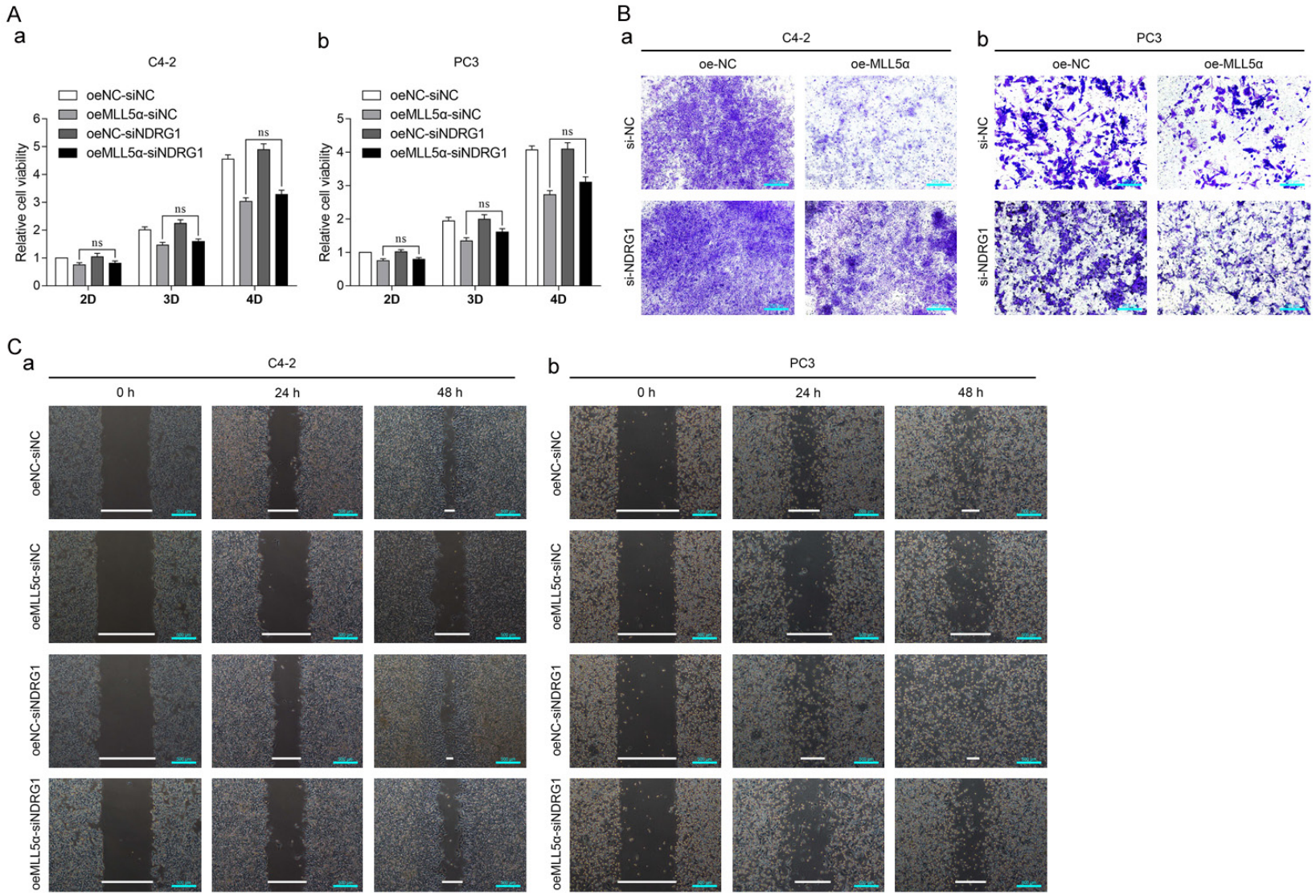

Figure 5. MLL5α suppresses PCa cell invasion and migration by activating AR/NDRG1 signaling. (A-C) MLL5α was overexpressed (oe-MLL5α/NC) in C4-2 (Aa, Ba, and Ca) and PC3 (Ab, Bb, and Cb) cells, and NDRG1 expression was then inhibited via transient transfection of siRNA (si-NDRG1/NC). A CCK-8 assay (A), Transwell assay (B), and wound healing assay (C) were performed. The results are presented as the means ± SEMs. ns $P > 0.05$.

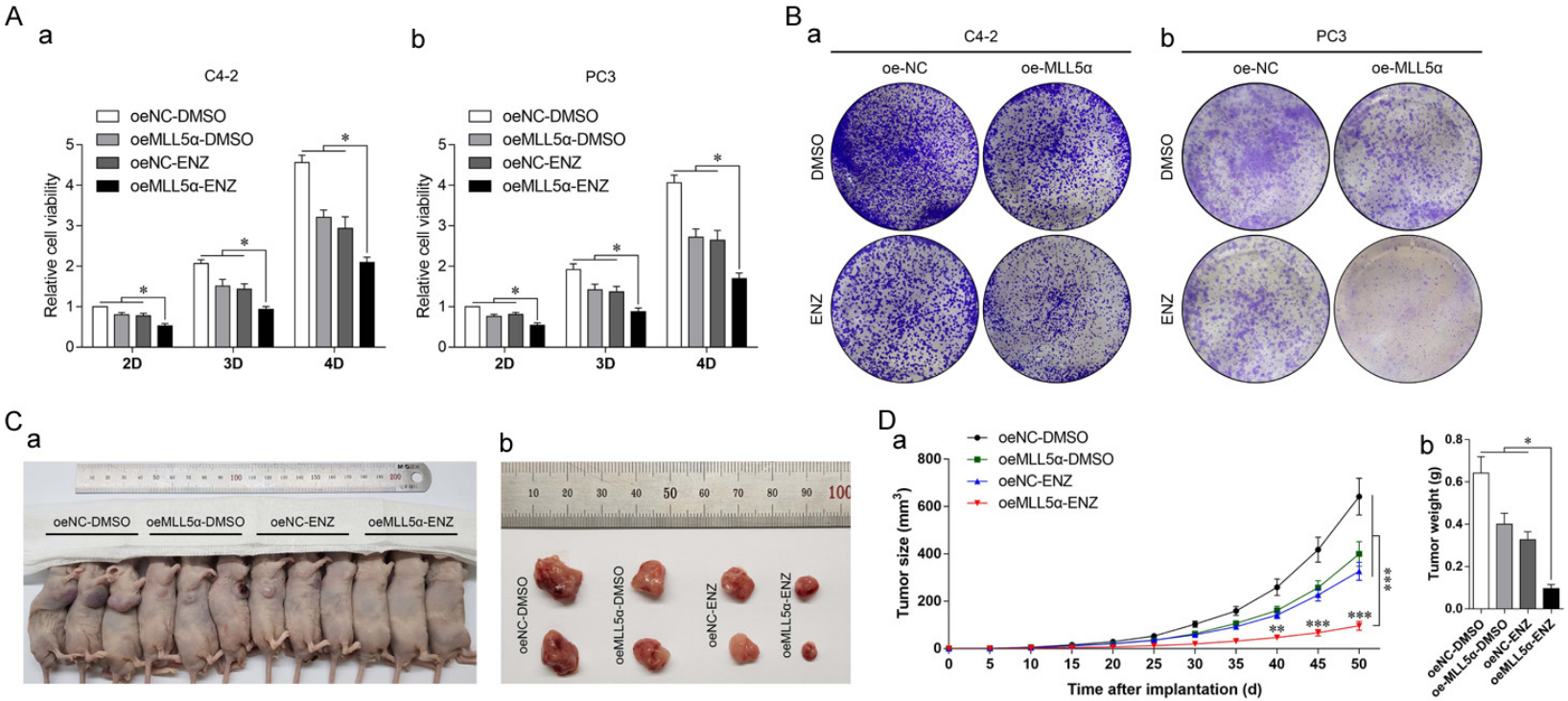
A
a
C4-2
oeNC-DMSO
oeMLL5α-DMSO
oeNC-ENZ
oeMLL5α-ENZ
Relative cell viability
2D
3D
4D
b
PC3
B
a
C4-2
oe-NC
oe-MLL5α
DMSO
ENZ
b
PC3
C
a
oeNC-DMSO
oeMLL5α-DMSO
oeNC-ENZ
oeMLL5α-ENZ
b
D
a
Tumor size (mm3)
Time after implantation (d)
b
Tumor weight (g)

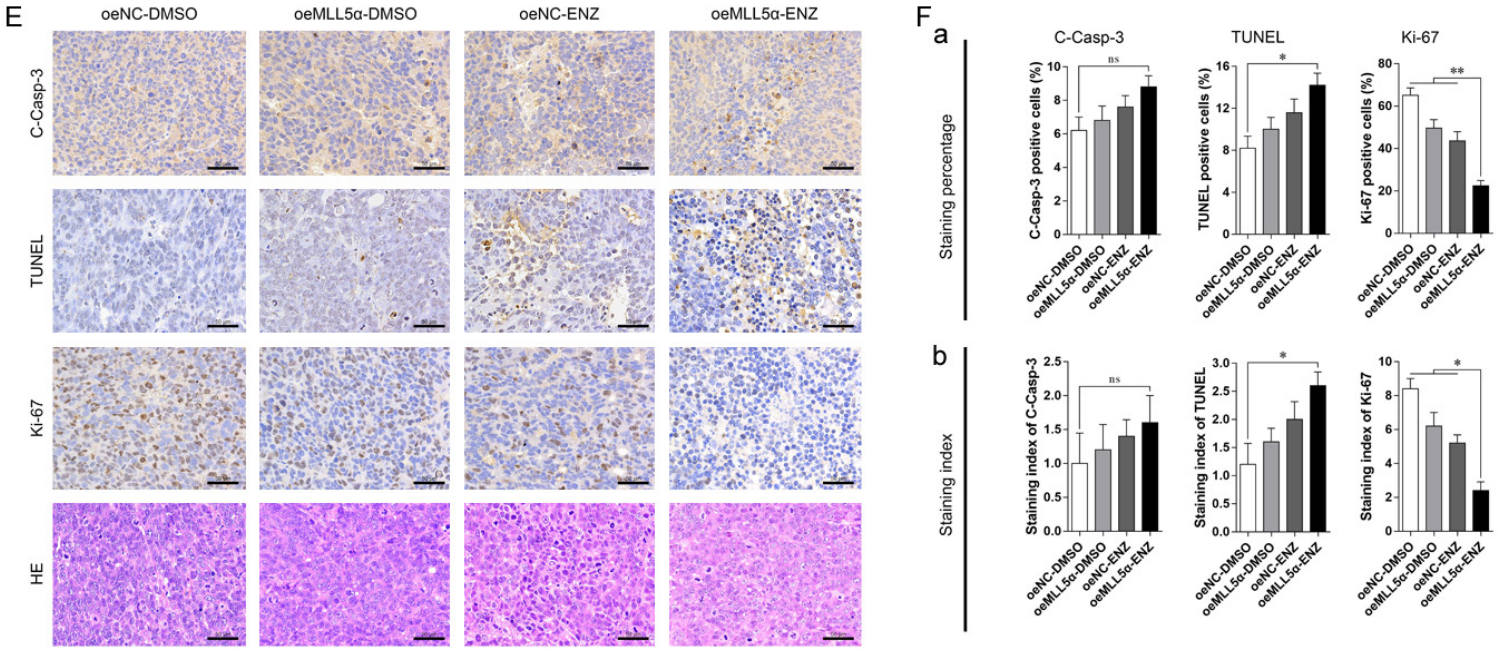

Figure 6. Overexpression of MLL5α promotes PCa cell sensitivity to ENZ treatment. (A and B) C4-2 (Aa and Ba) and PC3 (Ab and Bb) oe-MLL5α/NC cells were treated with 20 μM ENZ or the same volume of DMSO. A CCK-8 assay (A) and colony formation assay (B) were performed. The results are presented as the means ± SEMs. *P < 0.05. (C-F) Mice xenografted with C42-oe-MLL5α/NC cells were treated with 25 mg/kg/day ENZ or the same volume of DMSO and were randomly divided into four groups: oeNC-DMSO, oeMLL5α-DMSO, oeNC-ENZ, and oeMLL5α-ENZ. (C) Photographs of tumors on the fiftieth day after the inoculation of cells into the axilla of mice. (D) Tumor growth curves (a) and excised tumor weights (b) were quantitatively analyzed. The results are presented as the means ± SEMs. *P < 0.05, **P < 0.01 and ***P < 0.001. (E) Representative images of IHC staining for cleaved caspase-3 (C-Casp-3); Ki-67; TUNEL; and HE staining in each group. (F) Quantitative results of the staining percentage (a) and staining index (b) in each group. The results are presented as the means ± SEMs. ns P > 0.05, *P < 0.05, and **P < 0.01.

Table 1. Correlations of MLL5α expression and PCa patients' clinical characteristics

Clinicopathological parameters	Total (n = 45) (%)	MLL5α expression[a]		*P* value S-T[b]/M-W[c]/χ^{2}[d] test
		Low (%)	High (%)	
Age				0.876[b]
Median (IQR)	63 (61-68.5)	63 (60.75-68.25)	64 (61-69)	
Range (Min, Max)	55-74	57-74	55-73	
< 65	25 (55.6%)	12 (54.5%)	13 (56.5%)	0.894[d]
≥ 65	20 (44.4%)	10 (45.5%)	10 (43.5%)	
Total PSA (t-PSA)				0.496[c]
Median (IQR)	10.42 (7.56-21.6)	11.425 (7.275-35.5725)	9.94 (7.53-16.51)	
Range (Min, Max)	0.03-99.53	2.31-99.53	0.03-51.45	
< 4 ng/ml	3 (6.7%)	2 (9.1%)	1 (4.3%)	0.505[d]
4-10 ng/ml	18 (40.0%)	7 (31.8%)	11 (47.8%)	
> 10 ng/ml	24 (53.3%)	13 (59.1%)	11 (47.8%)	
Gleason score (GS)				
< 7	15 (33.3%)	4 (18.2%)	11 (47.8%)	0.083[d]
7	15 (33.3%)	8 (36.4%)	7 (30.4%)	
> 7	15 (33.3%)	10 (45.5%)	5 (21.7%)	
Clinical T-stage				
T2a	11 (24.4%)	3 (13.6%)	8 (34.8%)	0.031[d,*]
T2b	15 (33.3%)	5 (22.7%)	10 (43.5%)	
T2c	11 (24.4%)	9 (40.9%)	2 (8.7%)	
T3a or T3b	8 (17.8%)	5 (22.7%)	3 (13.0%)	
Lymph node metastasis				
N0	33 (73.3%)	13 (59.1%)	20 (87.0%)	0.035[d,*]
N1	12 (26.7%)	9 (40.9%)	3 (13.0%)	
Distant metastasis				
Mx	39 (86.7%)	18 (81.8%)	21 (91.3%)	0.619[d]
M1	6 (13.3%)	4 (18.2%)	2 (8.7%)	
TNM stage				
I-II	29 (64.4%)	12 (54.5%)	17 (73.9%)	0.175[d]
III-IV	16 (35.6%)	10 (45.5%)	6 (26.1%)	

*P < 0.05. [a]Median mRNA expression of MLL5α as cutoff. [b]*P* value (2-sided) of Student's T Test. [c]*P* value (2-sided) of Mann-Whitney U Test. [d]*P* value (2-sided) of Pearson Chi-Square Test or continuity correction of Chi-Square Test.

Kaplan-Meier survival and Cox regression analyses to determine the effects of MLL5, NDRG1, KLK3, and AR expression on patient prognosis (with the median reported expression value as the cutoff). The recurrence-free survival analysis results showed that patients with low expression levels of MLL5, NDRG1, and KLK3 tended to have poor prognoses for disease recurrence and higher HRs ($P(MC)_{MLL5}$ = 0.0571, $HR(MH)_{MLL5\ (low/high)}$ = 1.897 (0.981-3.667); $P(MC)_{NDRG1}$ = 0.0425, $HR(MH)_{NDRG1\ (low/high)}$ = 1.967 (1.023-3.783); $P(MC)_{KLK3}$ = 0.0497, $HR(MH)_{KLK3\ (low/high)}$ = 1.929 (1.001-3.719)), but no differences were found for the effect of AR expression on PCa patients' prognosis ($P(MC)_{AR}$ = 0.8276, $HR(MH)_{AR\ (low/high)}$ = 0.9298 (0.4827-1.791)) (**Figure 8Ba-d**). We also analyzed overall recurrence-free survival with overall survival follow-up time and found that the expression levels of MLL5, NDRG1, KLK3, and AR did not affect patients' survival prognoses (Supplementary Figure 2). However, only 11 of the 140 patients died during follow-up, and only 1 patient died of PCa.

Discussion

In this study, we found a novel protein, MLL5α, that epigenetically regulates AR/NDRG1 signaling through H3K4 methylation to suppress PCa progression. Our results provide the first evidence of the formation of an MLL5α-AR complex and its association with AREs in NDRG1 and KLK3 in PCa.

As an epigenetic regulator, MLL5 acts not only as a transcriptional activator by facilitating H3K4me [22, 23] but also as an epigenetic

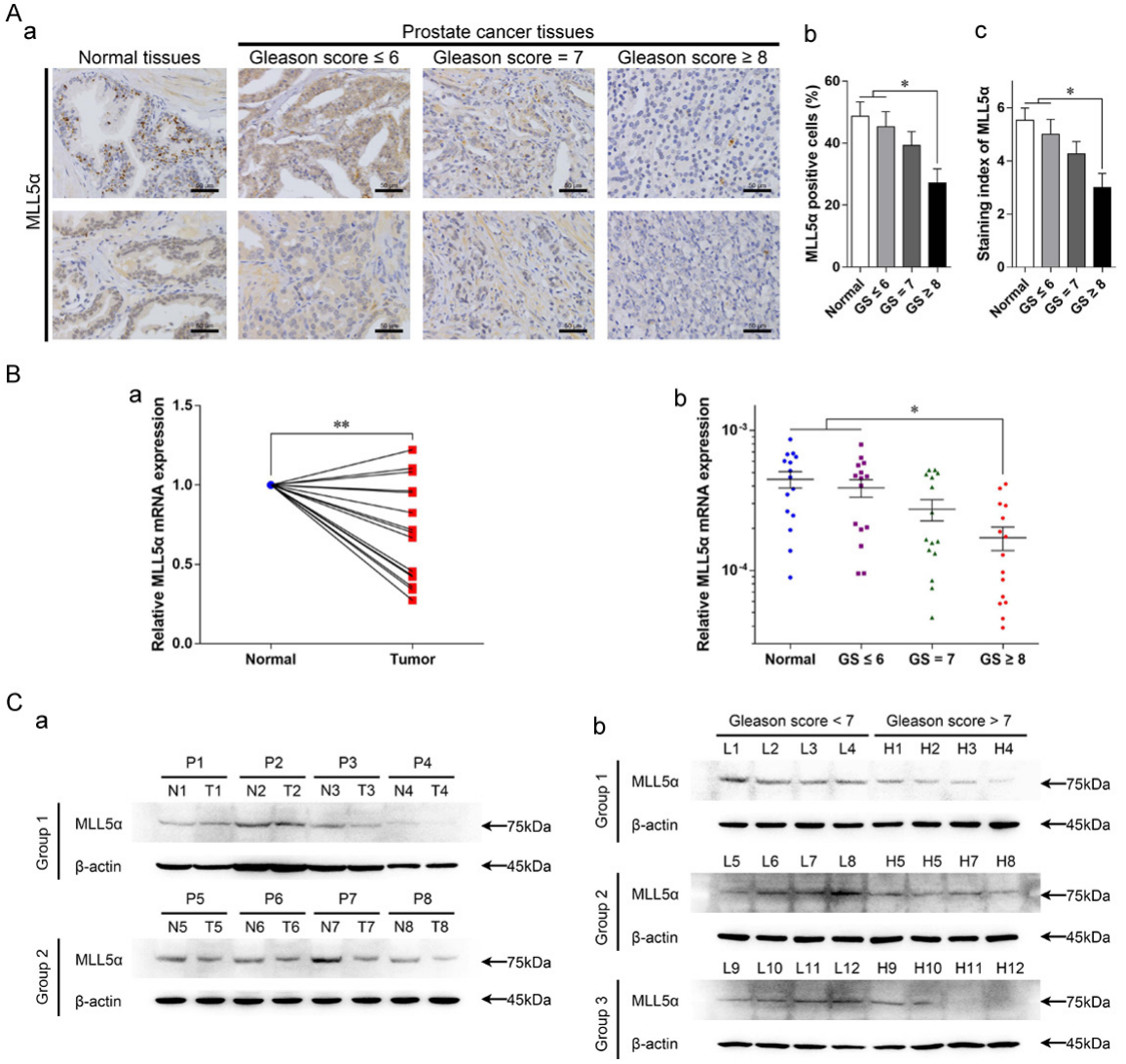

Figure 7. Low expression of MLL5α in advanced stages of PCa. PCa tissues were divided into 4 groups: normal tissue, GS ≤ 6, GS = 7, and GS ≥ 8. A. Representative images (a) of IHC for MLL5α in the four groups of PCa patients. Quantitative results of the staining percentage (b) and staining index (c) in each group. The results are presented as the means ± SEMs. *P < 0.05. B. Relative mRNA levels (normalized to those in adjacent normal tissues) of MLL5α in 15 PCa patients (a) and relative mRNA levels (normalized to those of 18S ribosomal RNA) in the four groups of PCa patients (b). The results are presented as the means ± SEMs. *P < 0.05 and **P < 0.01. C. MLL5α protein levels as determined via WB analysis in PCa patients compared to those in adjacent normal tissues (a) and MLL5α protein levels in the GS ≥ 8 group compared to those in the GS ≤ 6 group (b).

repressor (in glioblastoma cells) by repressing the histone 3 variant H3.3 [38]. These dual functions were based on specific cells, target genes, and the microenvironment. Stable expression of MLL5α is cooperatively regulated by OGlcNac Transferase (OGT) and Ubiquitin Specific Protease 7 (USP7) to enable its function as an epigenetic regulator through histone methylation [39]. In different PCa/hyperplasia cell lines (BPH-1, LNCaP, 22RV1, C4-2, and PC3), high expression of MLL5α and negligible expression of full-length MLL5 were found, and MLL5α was relatively highly expressed in AR-positive cell lines (LNCaP, 22RV1, and C4-2). Therefore, we considered MLL5α as an epigenetic regulator and further explored the relationship between MLL5α expression and AR transcriptional activity.

The function of MLL5α as a histone methylase is controversial [21-27, 38]; MLL5α was even suggested to repress H3K4me3 in glioblastoma multiforme (GBM) primary cultures [38]. Considering these opposite functions of ML-

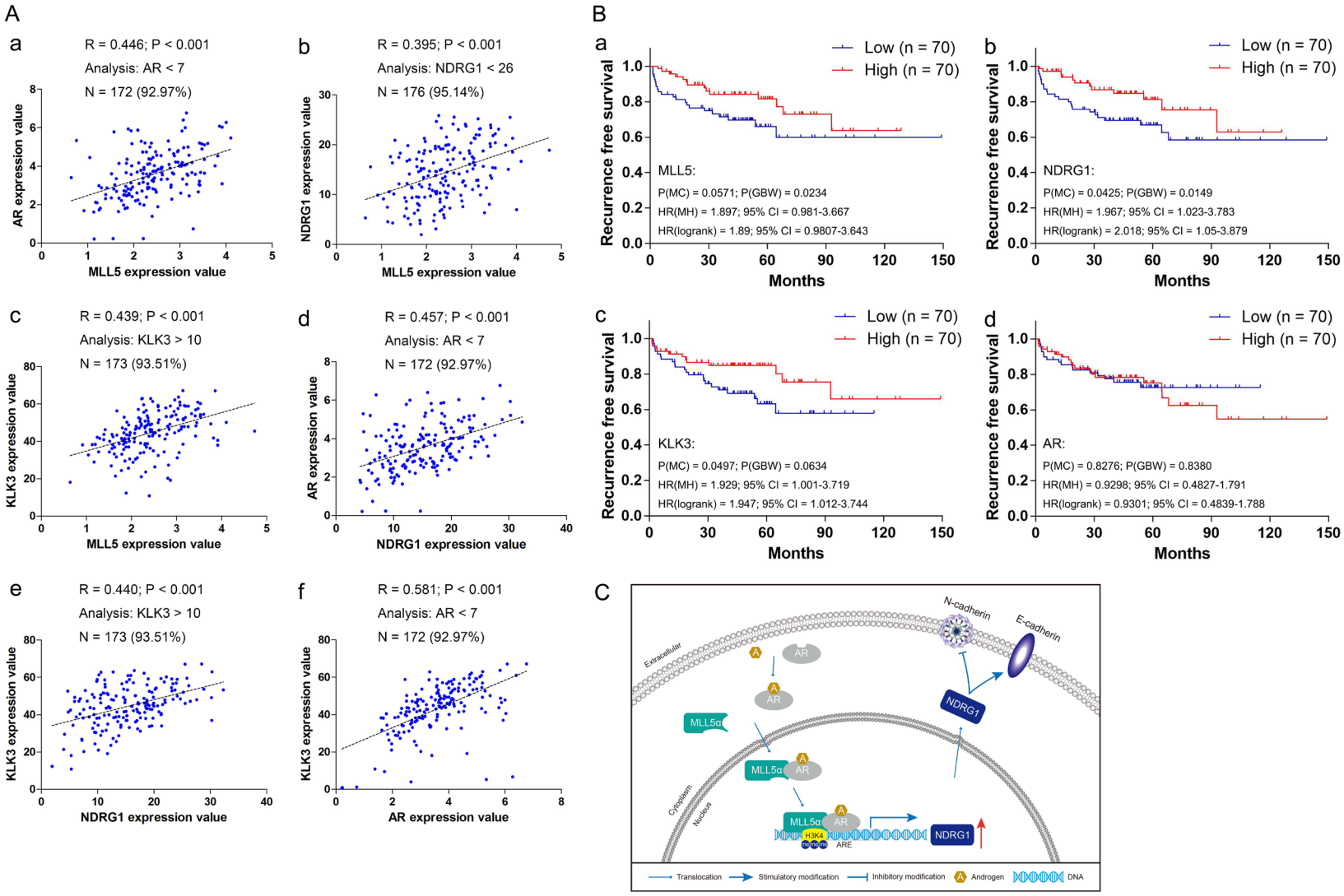

Figure 8. Low expression of MLL5 was associated with poor recurrence-free survival of PCa patients in the Taylor Prostate 3 database. A. The relationships between MLL5 and AR (a), MLL5 and NDRG1 (b), MLL5 and KLK3 (c), NDRG1 and AR (d), NDRG1 and KLK3 (e), and AR and KLK3 (f) were evaluated through analysis of the Taylor Prostate 3 database (R: correlation coefficient; N: number of analyzed samples (as a percentage of the total number of samples)). B. Kaplan-Meier survival curves and Cox regression model for the association between the expression of MLL5 (a), NDRG1 (b), KLK3 (c), and AR (d) and patients' recurrence-free survival (with the median reported expression value as the cutoff; P (MC): *P* value from the log-rank (Mantel-Cox) test; P (GBW): *P* value from the Gehan-Breslow-Wilcoxon test; HR(MH): hazard ratio (Mantel-Haenszel); HR (log-rank): hazard ratio (log-rank); 95% CI: 95% confidence interval of the HR in the Low/High groups). C. Potential mechanism by which MLL5α triggers AR/NDRG1 signaling.

L5α in a single cell line, we downregulated the expression of MLL5α in LNCaP cells and assessed the quantitative changes in global H3K4 methylation. Knockdown of MLL5α significantly reduced the levels of global H3K4me2 and H3K4me3, implying that MLL5α induces H3K4 methylation activity in PCa.

Knockdown of MLL5α induced the expression of neuroendocrine markers (CgA, Syn, and NSE), indicating potential transformation of ADPC to NEPC. In various PCa cells (LNCaP, C4-2, and PC3), MLL5α promoted AR, NDRG1, and E-cadherin expression and suppressed the expression of EMT markers (N-cadherin, Slug, Snail, Vimentin, and ZEB1), implying that the tendency of PCa to progress to CRPC is mediated through the potential relationship among MLL5α, NDRG1, and AR.

MLL5 was reported to be not only a cell cycle repressor by repressing cyclin A2 expression [25] but also a cell cycle promoter by activating E2F1 transcriptional activity and promoting G1/S and G2/M phase transitions [22, 40-42]. Because the role of MLL5α in PCa is not clearly defined, we regulated the expression of MLL5α in LNCaP, 22RV1, and C4-2 cells and assessed the effects of MLL5α on cell proliferation, invasion, and migration. Knockdown of MLL5α significantly promoted LNCaP cell proliferation and invasion, and overexpression of MLL5α suppressed the proliferation, invasion, and migration of 22RV1 and C4-2 cells. This result suggests the anticancer effect of MLL5α in PCa cells.

As a transcription factor, AR plays dual functions in the progression of PCa [43-47]. ADT drives PCa metastasis [48-50], EMT [51, 52], and neuroendocrine differentiation [53]. Though studies have documented AR as a PCa suppressor [3, 46, 51, 54, 55], the specific mechanism of ADT-induced PCa progression is largely unknown.

After ADT, repression of AR transcriptional activity may crucially affect the progression of PCa. Several AR target genes (such as NDRG1 [33, 34, 56] and PMEPA1 [34, 57, 58]) are tumor suppressors, and dysregulated expression of these genes induced by ADT is of considerable importance to PCa progression. Histone methylases and demethylases such as EZH2 [59-65] and LSD1 [65-68] were reported to function as both AR transcriptional co-activators and co-repressors on various target genes. Therefore, determining the function of novel AR co-activators in specific recognized target genes is important for investigating the mechanism of PCa progression.

In this study, we found a novel complex formed by MLL5α and AR. When we assessed the effect of MLL5α on AR transcriptional activity by evaluating representative AR target genes (PMEPA1, FGF8, NDRG1, KLK2, KLK3, TMPRSS, and IGF1R), we found that knockdown of MLL5α significantly reduced the expression of PMEPA1 (shNC-DHT:shMLL5α-DHT = 1:0.78), NDRG1 (shNC-DHT:shMLL5α-DHT = 1:0.26), and KLK3 (shNC-DHT:shMLL5α-DHT = 1:0.39). Considering their relative expression levels, NDRG1 and KLK3 were selected for further study as representatives of MLL5α-affected AR target genes. The ChIP assay results showed that 3 × Flag-tagged MLL5α directly recognized the AREs in NDRG1 and KLK3 and that DHT stimulation enhanced the binding efficiency. MLL5α also activated the transcriptional activity of the NDRG1 and KLK3 promoter regions via H3K4me3 recruitment and AR accumulation in the AREs in NDRG1 and KLK3. Based on these findings, we concluded that MLL5α promotes AR/NDRG1 signaling through H3K4me3 in AREs.

According to the results of clinical data analysis, KLK3, also called prostate-specific antigen (PSA), was found to be expressed at low levels in many patients diagnosed with aggressive PCa; thus, there may be another mechanism that promotes PCa progression without inducing PSA upregulation. To evaluate the function of MLL5α in suppressing PCa progression through AR/NDRG1 signaling, we downregulated the expression of NDRG1 in C4-2/PC3-oe-MLL5α/NC cells via siRNA and assessed cell proliferation, invasion, and migration. Downregulation of NDRG1 partially restored PCa cell invasion and migration suppressed by MLL5α but did not restore proliferation. Considering that the suppressive effects of MLL5α on PCa cell invasion and migration were related to AR/NDRG1 signaling, there may be other mechanisms by which MLL5α suppresses PCa cell proliferation. As mentioned above, MLL5α was suggested to act as a cell cycle suppressor by repressing cyclin A2 expression [25]. This mechanism may explain why MLL5α suppressed the proliferation of PCa cells.

Epigenetic reprogramming was reported to be a key regulator of the transition between CRPC and ADT sensitivity [62]. Regarding the histone lysine N-methyltransferase EZH2, studies have suggested that inhibition of EZH2 activates AR signaling and restores the sensitivity of CRPC cells to ENZ therapy [62, 69-71]. However, activating AR signaling to restore sensitivity to AR-targeted therapy is obviously contradictory. Thus, we aimed to evaluate the dual function of AR signaling. Because EZH2 has been reported to both activate [59, 60, 63] and repress [61, 62, 64, 65] AR transcriptional activity, we assumed that epigenetic regulators such as EZH2 and MLL5α may regulate AR transcriptional activity on specific target genes, allowing the selective activation or repression of distinct AR target genes in specific microenvironments. Knockdown of MLL5α in LNCaP cells resulted in a preference for the regulation of NDRG1 and KLK3 among representative AR target genes and promoted LNCaP cell proliferation and invasion. Synergistic antiproliferative effects of MLL5α and ENZ treatment were found in C4-2 and PC3 cells. An in vivo assay in a xenograft model also showed that overexpression of MLL5α enhanced ENZ sensitivity, as shown by the decreased tumor growth and increased tumor apoptosis. These results show the potential for CRPC to transition to ENZ sensitivity after overexpression of MLL5α in PCa cells.

A GS of ≥ 7 has been defined as a strong predictor of PCa aggressiveness [72, 73]. With this surrogate marker, we divided PCa tissues into three groups: GS < 7 (low GS group), GS = 7 (moderate GS group), and GS > 7 (high GS group). The MLL5α protein level was significantly lower in the high GS group than in the low GS and normal tissue groups. Low expression of MLL5 also indicated a poor recurrence-free survival prognosis (HR (MH) = 1.897, 95% CI = 0.981-3.667) of PCa patients in the Taylor Prostate 3 database, and the expression of MLL5 was positively correlated with the expression of AR, NDRG1, and KLK3. These conclusions were consistent with our previous results indicating that MLL5α has contradictory effects on PCa progression by triggering AR/NDRG1 signaling.

This study raised several points that warrant further research. First, MLL5α bound to AR and selectively activated AR target genes; however, the precise mechanism underlying this specific recognition was unclear. Second, MLL5α suppressed PCa cell proliferation independent of AR/NDRG1 signaling, but the molecular mechanism was undetermined.

Conclusions

In this study, we found that MLL5α suppressed PCa progression by activating AR/NDRG1 signaling. MLL5α directly binds with AR and recognizes the AREs in NDRG1 and KLK3 to activate their transcription via H3K4me3. MLL5α overexpression acts as a suppressor of tumor proliferation in PCa and promotes PCa sensitivity to ENZ treatment. Through this mechanism, MLL5α upregulation may be a treatment approach for PCa patients. In addition, MLL5α is expressed at lower levels in PCa tissues than in adjacent normal tissues, and MLL5α expression is inversely related to the GS and prognosis of PCa. Thus, MLL5α may be a biomarker for PCa progression.

Acknowledgements

This study was supported by a grant from the National Natural Science Foundation of China (81772698).

Disclosure of conflict of interest

None.

Address correspondence to: Xiaodong Zhang, Department of Urology, Beijing Chaoyang Hospital, Capital Medical University, Beijing 100020, China. E-mail: zhangxiaodong@bjcyh.com; Hao Ping, Department of Urology, Beijing Tongren Hospital, Capital Medical University, Beijing 100730, China. E-mail: haopingcyh@163.com

References

[1] Torre LA, Bray F, Siegel RL, Ferlay J, Lortet-Tieulent J and Jemal A. Global cancer statistics, 2012. CA Cancer J Clin 2015; 65: 87-108.

[2] Huang Y, Jiang X, Liang X and Jiang G. Molecular and cellular mechanisms of castration resistant prostate cancer. Oncol Lett 2018; 15: 6063-6076.

[3] Jia L, Wu D, Wang Y, You W, Wang Z, Xiao L, Cai G, Xu Z, Zou C, Wang F, Teoh JY, Ng CF, Yu S and Chan FL. Orphan nuclear receptor TLX contributes to androgen insensitivity in castration-resistant prostate cancer via its repression of

androgen receptor transcription. Oncogene 2018; 37: 3340-3355.
[4] Jennbacken K, Tesan T, Wang W, Gustavsson H, Damber JE and Welen K. N-cadherin increases after androgen deprivation and is associated with metastasis in prostate cancer. Endocr Relat Cancer 2010; 17: 469-479.
[5] Mendiratta P, Mostaghel E, Guinney J, Tewari AK, Porrello A, Barry WT, Nelson PS and Febbo PG. Genomic strategy for targeting therapy in castration-resistant prostate cancer. J Clin Oncol 2009; 27: 2022-2029.
[6] Masai M, Sumiya H, Akimoto S, Yatani R, Chang CS, Liao SS and Shimazaki J. Immunohistochemical study of androgen receptor in benign hyperplastic and cancerous human prostates. Prostate 1990; 17: 293-300.
[7] Segawa N, Mori I, Utsunomiya H, Nakamura M, Nakamura Y, Shan L, Kakudo K and Katsuoka Y. Prognostic significance of neuroendocrine differentiation, proliferation activity and androgen receptor expression in prostate cancer. Pathol Int 2001; 51: 452-459.
[8] Chodak GW, Kranc DM, Puy LA, Takeda H, Johnson K and Chang C. Nuclear localization of androgen receptor in heterogeneous samples of normal, hyperplastic and neoplastic human prostate. J Urol 1992; 147: 798-803.
[9] Ruizeveld de Winter JA, Janssen PJ, Sleddens HM, Verleun-Mooijman MC, Trapman J, Brinkmann AO, Santerse AB, Schroder FH and van der Kwast TH. Androgen receptor status in localized and locally progressive hormone refractory human prostate cancer. Am J Pathol 1994; 144: 735-746.
[10] Li R, Wheeler T, Dai H, Frolov A, Thompson T and Ayala G. High level of androgen receptor is associated with aggressive clinicopathologic features and decreased biochemical recurrence-free survival in prostate: cancer patients treated with radical prostatectomy. Am J Surg Pathol 2004; 28: 928-934.
[11] Takeda H, Akakura K, Masai M, Akimoto S, Yatani R and Shimazaki J. Androgen receptor content of prostate carcinoma cells estimated by immunohistochemistry is related to prognosis of patients with stage D2 prostate carcinoma. Cancer 1996; 77: 934-940.
[12] Pertschuk LP, Schaeffer H, Feldman JG, Macchia RJ, Kim YD, Eisenberg K, Braithwaite LV, Axiotis CA, Prins G and Green GL. Immunostaining for prostate cancer androgen receptor in paraffin identifies a subset of men with a poor prognosis. Lab Invest 1995; 73: 302-305.
[13] Komiya A, Yasuda K, Watanabe A, Fujiuchi Y, Tsuzuki T and Fuse H. The prognostic significance of loss of the androgen receptor and neuroendocrine differentiation in prostate biopsy specimens among castration-resistant prostate cancer patients. Mol Clin Oncol 2013; 1: 257-262.
[14] Beltran H, Rickman DS, Park K, Chae SS, Sboner A, MacDonald TY, Wang Y, Sheikh KL, Terry S, Tagawa ST, Dhir R, Nelson JB, de la Taille A, Allory Y, Gerstein MB, Perner S, Pienta KJ, Chinnaiyan AM, Wang Y, Collins CC, Gleave ME, Demichelis F, Nanus DM and Rubin MA. Molecular characterization of neuroendocrine prostate cancer and identification of new drug targets. Cancer Discov 2011; 1: 487-495.
[15] Beltran H, Prandi D, Mosquera JM, Benelli M, Puca L, Cyrta J, Marotz C, Giannopoulou E, Chakravarthi BV, Varambally S, Tomlins SA, Nanus DM, Tagawa ST, Van Allen EM, Elemento O, Sboner A, Garraway LA, Rubin MA and Demichelis F. Divergent clonal evolution of castration-resistant neuroendocrine prostate cancer. Nat Med 2016; 22: 298-305.
[16] Kouzarides T. Chromatin modifications and their function. Cell 2007; 128: 693-705.
[17] Jenuwein T and Allis CD. Translating the histone code. Science 2001; 293: 1074-1080.
[18] Krogan NJ, Kim M, Tong A, Golshani A, Cagney G, Canadien V, Richards DP, Beattie BK, Emili A, Boone C, Shilatifard A, Buratowski S and Greenblatt J. Methylation of histone H3 by Set2 in Saccharomyces cerevisiae is linked to transcriptional elongation by RNA polymerase II. Mol Cell Biol 2003; 23: 4207-4218.
[19] Strahl BD and Allis CD. The language of covalent histone modifications. Nature 2000; 403: 41-45.
[20] Morishita M, Mevius D and di Luccio E. In vitro histone lysine methylation by NSD1, NSD2/MMSET/WHSC1 and NSD3/WHSC1L. BMC Struct Biol 2014; 14: 25.
[21] Zhang X, Novera W, Zhang Y and Deng LW. MLL5 (KMT2E): structure, function, and clinical relevance. Cell Mol Life Sci 2017; 74: 2333-2344.
[22] Zhou P, Wang Z, Yuan X, Zhou C, Liu L, Wan X, Zhang F, Ding X, Wang C, Xiong S, Wang Z, Yuan J, Li Q and Zhang Y. Mixed lineage leukemia 5 (MLL5) protein regulates cell cycle progression and E2F1-responsive gene expression via association with host cell factor-1 (HCF-1). J Biol Chem 2013; 288: 17532-17543.
[23] Ali M, Rincon-Arano H, Zhao W, Rothbart SB, Tong Q, Parkhurst SM, Strahl BD, Deng LW, Groudine M and Kutateladze TG. Molecular basis for chromatin binding and regulation of MLL5. Proc Natl Acad Sci U S A 2013; 110: 11296-11301.
[24] Fujiki R, Chikanishi T, Hashiba W, Ito H, Takada I, Roeder RG, Kitagawa H and Kato S. GlcNAcylation of a histone methyltransferase in retinoic-acid-induced granulopoiesis. Nature 2009; 459: 455-459.

[25] Sebastian S, Sreenivas P, Sambasivan R, Cheedipudi S, Kandalla P, Pavlath GK and Dhawan J. MLL5, a trithorax homolog, indirectly regulates H3K4 methylation, represses cyclin A2 expression, and promotes myogenic differentiation. Proc Natl Acad Sci U S A 2009; 106: 4719-4724.

[26] Mas-Y-Mas S, Barbon M, Teyssier C, Demene H, Carvalho JE, Bird LE, Lebedev A, Fattori J, Schubert M, Dumas C, Bourguet W and le Maire A. The human mixed lineage leukemia 5 (MLL5), a sequentially and structurally divergent SET domain-containing protein with no intrinsic catalytic activity. PLoS One 2016; 11: e0165139.

[27] Lemak A, Yee A, Wu H, Yap D, Zeng H, Dombrovski L, Houliston S, Aparicio S and Arrowsmith CH. Solution NMR structure and histone binding of the PHD domain of human MLL5. PLoS One 2013; 8: e77020.

[28] Park KC, Menezes SV, Kalinowski DS, Sahni S, Jansson PJ, Kovacevic Z and Richardson DR. Identification of differential phosphorylation and sub-cellular localization of the metastasis suppressor, NDRG1. Biochim Biophys Acta Mol Basis Dis 2018; 1864: 2644-2663.

[29] Lee JE and Kim JH. Valproic acid inhibits the invasion of PC3 prostate cancer cells by up-regulating the metastasis suppressor protein NDRG1. Genet Mol Biol 2015; 38: 527-533.

[30] Li Y, Pan P, Qiao P and Liu R. Downregulation of N-myc downstream regulated gene 1 caused by the methylation of CpG islands of NDRG1 promoter promotes proliferation and invasion of prostate cancer cells. Int J Oncol 2015; 47: 1001-1008.

[31] Liu R, Li J, Teng Z, Zhang Z and Xu Y. Overexpressed microRNA-182 promotes proliferation and invasion in prostate cancer PC-3 cells by down-regulating N-myc downstream regulated gene 1 (NDRG1). PLoS One 2013; 8: e68982.

[32] Song Y, Oda Y, Hori M, Kuroiwa K, Ono M, Hosoi F, Basaki Y, Tokunaga S, Kuwano M, Naito S and Tsuneyoshi M. N-myc downstream regulated gene-1/Cap43 may play an important role in malignant progression of prostate cancer, in its close association with E-cadherin. Hum Pathol 2010; 41: 214-222.

[33] Kim KH, Dobi A, Shaheduzzaman S, Gao CL, Masuda K, Li H, Drukier A, Gu Y, Srikantan V, Rhim JS and Srivastava S. Characterization of the androgen receptor in a benign prostate tissue-derived human prostate epithelial cell line: RC-165N/human telomerase reverse transcriptase. Prostate Cancer Prostatic Dis 2007; 10: 30-38.

[34] Masuda K, Werner T, Maheshwari S, Frisch M, Oh S, Petrovics G, May K, Srikantan V, Srivastava S and Dobi A. Androgen receptor binding sites identified by a GREF_GATA model. J Mol Biol 2005; 353: 763-771.

[35] Jeon HG, Jeong IG, Bae J, Lee JW, Won JK, Paik JH, Kim HH, Lee SE and Lee E. Expression of Ki-67 and COX-2 in patients with upper urinary tract urothelial carcinoma. Urology 2010; 76: 513, e517-512.

[36] Wang L, Li J, Hou J, Li M, Cui X, Li S, Yu X, Zhang Z, Liang W, Jiang J, Pang L, Chen Y, Zhao J and Li F. p53 expression but not p16(INK4A) correlates with human papillomavirus-associated esophageal squamous cell carcinoma in Kazakh population. Infect Agent Cancer 2016; 11: 19.

[37] Wang L, Zhang Z, Yu X, Huang X, Liu Z, Chai Y, Yang L, Wang Q, Li M, Zhao J, Hou J and Li F. Unbalanced YAP-SOX9 circuit drives stemness and malignant progression in esophageal squamous cell carcinoma. Oncogene 2019; 38: 2042-2055.

[38] Gallo M, Coutinho FJ, Vanner RJ, Gayden T, Mack SC, Murison A, Remke M, Li R, Takayama N, Desai K, Lee L, Lan X, Park NI, Barsyte-Lovejoy D, Smil D, Sturm D, Kushida MM, Head R, Cusimano MD, Bernstein M, Clarke ID, Dick JE, Pfister SM, Rich JN, Arrowsmith CH, Taylor MD, Jabado N, Bazett-Jones DP, Lupien M and Dirks PB. MLL5 orchestrates a cancer self-renewal state by repressing the histone variant H3.3 and globally reorganizing chromatin. Cancer Cell 2015; 28: 715-729.

[39] Ding X, Jiang W, Zhou P, Liu L, Wan X, Yuan X, Wang X, Chen M, Chen J, Yang J, Kong C, Li B, Peng C, Wong CC, Hou F and Zhang Y. Mixed lineage leukemia 5 (MLL5) protein stability is cooperatively regulated by O-GlcNac transferase (OGT) and ubiquitin specific protease 7 (USP7). PLoS One 2015; 10: e0145023.

[40] Liu J, Wang XN, Cheng F, Liou YC and Deng LW. Phosphorylation of mixed lineage leukemia 5 by CDC2 affects its cellular distribution and is required for mitotic entry. J Biol Chem 2010; 285: 20904-20914.

[41] Cheng F, Liu J, Zhou SH, Wang XN, Chew JF and Deng LW. RNA interference against mixed lineage leukemia 5 resulted in cell cycle arrest. Int J Biochem Cell Biol 2008; 40: 2472-2481.

[42] Cheng F, Liu J, Teh C, Chong SW, Korzh V, Jiang YJ and Deng LW. Camptothecin-induced down-regulation of MLL5 contributes to the activation of tumor suppressor p53. Oncogene 2011; 30: 3599-3611.

[43] Chang C, Saltzman A, Yeh S, Young W, Keller E, Lee HJ, Wang C and Mizokami A. Androgen receptor: an overview. Crit Rev Eukaryot Gene Expr 1995; 5: 97-125.

[44] de Launoit Y, Veilleux R, Dufour M, Simard J and Labrie F. Characteristics of the biphasic action of androgens and of the potent antiproliferative effects of the new pure antiestrogen EM-139 on cell cycle kinetic parameters in LNCaP human prostatic cancer cells. Cancer Res 1991; 51: 5165-5170.

[45] Huggins C and Hodges CV. Studies on prostatic cancer. I. The effect of castration, of estrogen and androgen injection on serum phosphatases in metastatic carcinoma of the prostate. CA Cancer J Clin 1972; 22: 232-240.
[46] Niu Y, Chang TM, Yeh S, Ma WL, Wang YZ and Chang C. Differential androgen receptor signals in different cells explain why androgen-deprivation therapy of prostate cancer fails. Oncogene 2010; 29: 3593-3604.
[47] Singer EA, Golijanin DJ and Messing EM. Androgen deprivation therapy for advanced prostate cancer: why does it fail and can its effects be prolonged? Can J Urol 2008; 15: 4381-4387.
[48] Chen WY, Tsai YC, Siu MK, Yeh HL, Chen CL, Yin JJ, Huang J and Liu YN. Inhibition of the androgen receptor induces a novel tumor promoter, ZBTB46, for prostate cancer metastasis. Oncogene 2017; 36: 6213-6224.
[49] Qin J, Lee HJ, Wu SP, Lin SC, Lanz RB, Creighton CJ, DeMayo FJ, Tsai SY and Tsai MJ. Androgen deprivation-induced NCoA2 promotes metastatic and castration-resistant prostate cancer. J Clin Invest 2014; 124: 5013-5026.
[50] Chen J, Li L, Yang Z, Luo J, Yeh S and Chang C. Androgen-deprivation therapy with enzalutamide enhances prostate cancer metastasis via decreasing the EPHB6 suppressor expression. Cancer Lett 2017; 408: 155-163.
[51] Sun Y, Wang BE, Leong KG, Yue P, Li L, Jhunjhunwala S, Chen D, Seo K, Modrusan Z, Gao WQ, Settleman J and Johnson L. Androgen deprivation causes epithelial-mesenchymal transition in the prostate: implications for androgen-deprivation therapy. Cancer Res 2012; 72: 527-536.
[52] Tsai YC, Chen WY, Abou-Kheir W, Zeng T, Yin JJ, Bahmad H, Lee YC and Liu YN. Androgen deprivation therapy-induced epithelial-mesenchymal transition of prostate cancer through downregulating SPDEF and activating CCL2. Biochim Biophys Acta Mol Basis Dis 2018; 1864: 1717-1727.
[53] Chen WY, Zeng T, Wen YC, Yeh HL, Jiang KC, Chen WH, Zhang Q, Huang J and Liu YN. Androgen deprivation-induced ZBTB46-PTGS1 signaling promotes neuroendocrine differentiation of prostate cancer. Cancer Lett 2019; 440-441: 35-46.
[54] Niu Y, Altuwaijri S, Yeh S, Lai KP, Yu S, Chuang KH, Huang SP, Lardy H and Chang C. Targeting the stromal androgen receptor in primary prostate tumors at earlier stages. Proc Natl Acad Sci U S A 2008; 105: 12188-12193.
[55] Niu Y, Altuwaijri S, Lai KP, Wu CT, Ricke WA, Messing EM, Yao J, Yeh S and Chang C. Androgen receptor is a tumor suppressor and proliferator in prostate cancer. Proc Natl Acad Sci U S A 2008; 105: 12182-12187.
[56] Sharma A, Mendonca J, Ying J, Kim HS, Verdone JE, Zarif JC, Carducci M, Hammers H, Pienta KJ and Kachhap S. The prostate metastasis suppressor gene NDRG1 differentially regulates cell motility and invasion. Mol Oncol 2017; 11: 655-669.
[57] Xu LL, Shanmugam N, Segawa T, Sesterhenn IA, McLeod DG, Moul JW and Srivastava S. A novel androgen-regulated gene, PMEPA1, located on chromosome 20q13 exhibits high level expression in prostate. Genomics 2000; 66: 257-263.
[58] Li H, Mohamed AA, Sharad S, Umeda E, Song Y, Young D, Petrovics G, McLeod DG, Sesterhenn IA, Sreenath T, Dobi A and Srivastava S. Silencing of PMEPA1 accelerates the growth of prostate cancer cells through AR, NEDD4 and PTEN. Oncotarget 2015; 6: 15137-15149.
[59] Kim J, Lee Y, Lu X, Song B, Fong KW, Cao Q, Licht JD, Zhao JC and Yu J. Polycomb- and methylation-independent roles of EZH2 as a transcription activator. Cell Rep 2018; 25: 2808-2820, e2804.
[60] Liu Q, Wang G, Li Q, Jiang W, Kim JS, Wang R, Zhu S, Wang X, Yan L, Yi Y, Zhang L, Meng Q, Li C, Zhao D, Qiao Y, Li Y, Gursel DB, Chinnaiyan AM, Chen K and Cao Q. Polycomb group proteins EZH2 and EED directly regulate androgen receptor in advanced prostate cancer. Int J Cancer 2019; 145: 415-426.
[61] Dardenne E, Beltran H, Benelli M, Gayvert K, Berger A, Puca L, Cyrta J, Sboner A, Noorzad Z, MacDonald T, Cheung C, Yuen KS, Gao D, Chen Y, Eilers M, Mosquera JM, Robinson BD, Elemento O, Rubin MA, Demichelis F and Rickman DS. N-Myc Induces an EZH2-mediated transcriptional program driving neuroendocrine prostate cancer. Cancer Cell 2016; 30: 563-577.
[62] Xiao L, Tien JC, Vo J, Tan M, Parolia A, Zhang Y, Wang L, Qiao Y, Shukla S, Wang X, Zheng H, Su F, Jing X, Luo E, Delekta A, Juckette KM, Xu A, Cao X, Alva AS, Kim Y, MacLeod AR and Chinnaiyan AM. Epigenetic reprogramming with antisense oligonucleotides enhances the effectiveness of androgen receptor inhibition in Castration-resistant prostate cancer. Cancer Res 2018; 78: 5731-5740.
[63] Xu K, Wu ZJ, Groner AC, He HH, Cai C, Lis RT, Wu X, Stack EC, Loda M, Liu T, Xu H, Cato L, Thornton JE, Gregory RI, Morrissey C, Vessella RL, Montironi R, Magi-Galluzzi C, Kantoff PW, Balk SP, Liu XS and Brown M. EZH2 oncogenic activity in castration-resistant prostate cancer cells is Polycomb-independent. Science 2012; 338: 1465-1469.
[64] Cho S, Park JS and Kang YK. AGO2 and SETDB1 cooperate in promoter-targeted transcriptional silencing of the androgen receptor gene. Nucleic Acids Res 2014; 42: 13545-13556.

[65] Gritsina G, Gao WQ and Yu J. Transcriptional repression by androgen receptor: roles in castration-resistant prostate cancer. Asian J Androl 2019; 21: 215-223.
[66] Metzger E, Wissmann M, Yin N, Muller JM, Schneider R, Peters AH, Gunther T, Buettner R and Schule R. LSD1 demethylates repressive histone marks to promote androgen-receptor-dependent transcription. Nature 2005; 437: 436-439.
[67] Wissmann M, Yin N, Muller JM, Greschik H, Fodor BD, Jenuwein T, Vogler C, Schneider R, Gunther T, Buettner R, Metzger E and Schule R. Cooperative demethylation by JMJD2C and LSD1 promotes androgen receptor-dependent gene expression. Nat Cell Biol 2007; 9: 347-353.
[68] Cai C, He HH, Chen S, Coleman I, Wang H, Fang Z, Chen S, Nelson PS, Liu XS, Brown M and Balk SP. Androgen receptor gene expression in prostate cancer is directly suppressed by the androgen receptor through recruitment of lysine-specific demethylase 1. Cancer Cell 2011; 20: 457-471.
[69] Ku SY, Rosario S, Wang Y, Mu P, Seshadri M, Goodrich ZW, Goodrich MM, Labbe DP, Gomez EC, Wang J, Long HW, Xu B, Brown M, Loda M, Sawyers CL, Ellis L and Goodrich DW. Rb1 and Trp53 cooperate to suppress prostate cancer lineage plasticity, metastasis, and antiandrogen resistance. Science 2017; 355: 78-83.
[70] Bai Y, Zhang Z, Cheng L, Wang R, Chen X, Kong Y, Feng F, Ahmad N, Li L and Liu X. Inhibition of enhancer of zeste homolog 2 (EZH2) overcomes enzalutamide resistance in castration-resistant prostate cancer. J Biol Chem 2019; 294: 9911-9923.
[71] Wang HJ, Pochampalli M, Wang LY, Zou JX, Li PS, Hsu SC, Wang BJ, Huang SH, Yang P, Yang JC, Chu CY, Hsieh CL, Sung SY, Li CF, Tepper CG, Ann DK, Gao AC, Evans CP, Izumiya Y, Chuu CP, Wang WC, Chen HW and Kung HJ. KDM8/JMJD5 as a dual coactivator of AR and PKM2 integrates AR/EZH2 network and tumor metabolism in CRPC. Oncogene 2019; 38: 17-32.
[72] Eggener SE, Scardino PT, Walsh PC, Han M, Partin AW, Trock BJ, Feng Z, Wood DP, Eastham JA, Yossepowitch O, Rabah DM, Kattan MW, Yu C, Klein EA and Stephenson AJ. Predicting 15-year prostate cancer specific mortality after radical prostatectomy. J Urol 2011; 185: 869-875.
[73] Kozminski MA, Tomlins S, Cole A, Singhal U, Lu L, Skolarus TA, Palapattu GS, Montgomery JS, Weizer AZ, Mehra R, Hollenbeck BK, Miller DC, He C, Feng FY and Morgan TM. Standardizing the definition of adverse pathology for lower risk men undergoing radical prostatectomy. Urol Oncol 2016; 34: 415, e411-416.

Supplementary Table 1. Information of MLL5α related sequences and vectors

Name	Sequences		Vector
sh-MLL5α	ATGCTGAGAGAACAGTTTGAA sence (5'-3')	TTCAAACTGTTCTCTCAGCAT antisence (5'-3')	pSGLV-H1-GFP-puromycin
si-NDRG1	AACCUGCUACAACCCCCUCTT sence (5'-3')	GAGGGGGUUGUAGCAGGUUTT antisence (5'-3')	-
oe-MLL5α	NM_018682(1-609aa)-3flag		Ubi-MCS-SV40-EGFP-IRES-puromycin

Supplementary Table 2. Oligonucleotide primers of AR/NDRG1 relative genes

Gene	Forward	Reverse
MLL5α	TCCTCGGTTCCTGGTGAAGA	AACCCCGTTATGTGCTCGAC
AR	CTACATCAAGGAACTCGATCGT	CATGTGTGACTTGATTAGCAGG
NDRG1	GAAAAGCATTATTGGCATGGGA	CACAAGGGTTCACGTTGATAAG
GAPDH	TGACTTCAACAGCGACACCCA	CACCCTGTTGCTGTAGCCAAA

Supplementary Table 3. Oligonucleotide primers of androgen receptor-responsive genes

Gene	Forward	Reverse
PMEPA1	CATGATCCCCGAGCTGCT	TGATCTGAACAAACTCCAGCTCC
FGF8	CAACTCTACAGCCGCACCAGC	TGCTCTTGGCGATCAGCTTC
GREB1	AAGGAGGGCTGGAAACAAAT	CATTGTGGCCATTGTCATCT
NDRG1	GAAAAGCATTATTGGCATGGGA	CACAAGGGTTCACGTTGATAAG
KLK2	GCTGCCCATTGCCTAAAGAAG	TGGGAAGCTGTGGCTGACA
KLK3	CACCTGCTCGGGTGATTCTG	CCACTTCCGGTAATGCACCA
TMPRSS2	GGACAGTGTGCACCTCAAAGA	TTGCTGCCCATGAACTTCC
IGF1R	GGGCCATCAGGATTGAGAAA	CACAGGCCGTGTCGTTGTCA
18S	AAACGGCTACCACATCCA	CACCAGACTTGCCCCTCCA

Supplementary Table 4. Histone methylation relative antibodies information

Protein	Brand	NO.
H3K4me1	CST	#5326
H3K4me2	CST	#9725
H3K4me3	Abcam	ab8580
H3K9me2/3	CST	#5327
Histone H3	CST	#4499

Supplementary Table 5. Relative antibodies information

Protein	Brand	NO.
MLL5	Abcam	ab75339
MLL5α	Abgent	AP14173a
AR	Abcam	ab74272
NDRG1	CST	#9485
N-Cadherin	Abcam	ab18203
E-cadherin	CST	#3195
ZEB1	CST	#3396
Slug	CST	#9585
Snail	CST	#3879
Vimentin	CST	#5741
CgA	Abcam	ab15160
NSE	Abcam	ab79757
Syn	Abcam	ab32127
Ki-67	CST	#9449
Cleaved Caspase-3	CST	#9661
β-actin	CST	#3700

Supplementary Table 6. Co-IP assay related information of antibodies

Protein	Brand	NO.	Source
AR	Abcam	ab74272	rabbit
IgG	CST	#2729	rabbit
Flag	Sigma-Aldrich	F1804	mouse
MLL5α	Abgent	AP14173a	rabbit

Supplementary Table 7. ChIP assay related Oligonucleotide primers

Gene	Forward	Reverse	Region
NDRG1	GCCACCTGGGTAGCTTTGTA	AGAGGAGCCGCCAAATTAAA	-1066~-928
KLK3	GGGATCAGGGAGTCTCACAA	GCTAGCACTTGCTGTTCTGC	-393~-153

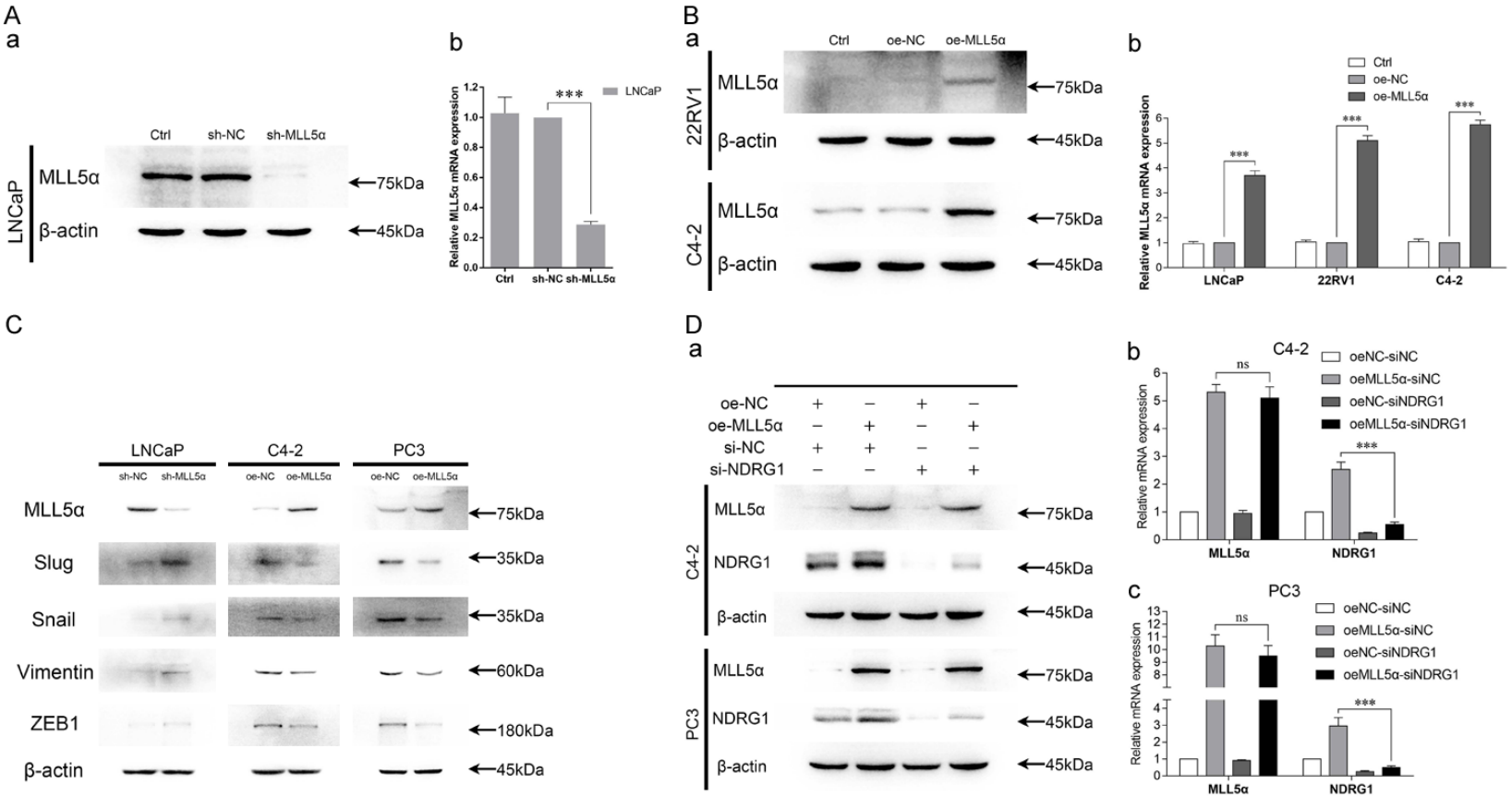

Supplementary Figure 1. Verification of the MLL5α regulating efficiency and MLL5α-affected markers. A. Expression of MLL5α was stably downregulated in LNCaP cells via lentiviral transduction (containing MLL5α-specific shRNA), and MLL5α protein levels (a) and mRNA levels (b) were assessed via WB and qPCR analyses. The results are presented as the means ± SEMs. ***P < 0.001. B. MLL5α was stably overexpressed in 22RV1 and C4-2 cells, and protein levels were assessed via WB analysis (a). MLL5α was overexpressed in LNCaP, 22RV1, and C4-2 cells, and mRNA levels were assessed via qPCR analysis (b). The results are presented as the means ± SEMs. ***P < 0.001. C. The expression of MLL5α was downregulated in LNCaP cells (sh-NC and sh-MLL5α) and was upregulated in C4-2 and PC3 cells (oe-NC and oe-MLL5α). WB was performed with EMT markers. D. MLL5α was stably overexpressed in C4-2 and PC3 cells, and the expression of NDRG1 was then knocked down via siRNA transfection. Protein levels in C4-2 and PC3 (a) cells were assessed via WB analysis, and mRNA levels in C4-2 (b) and PC3 (c) cells were assessed via qPCR analysis. The results are presented as the means ± SEMs. ns P > 0.05 and ***P < 0.001.

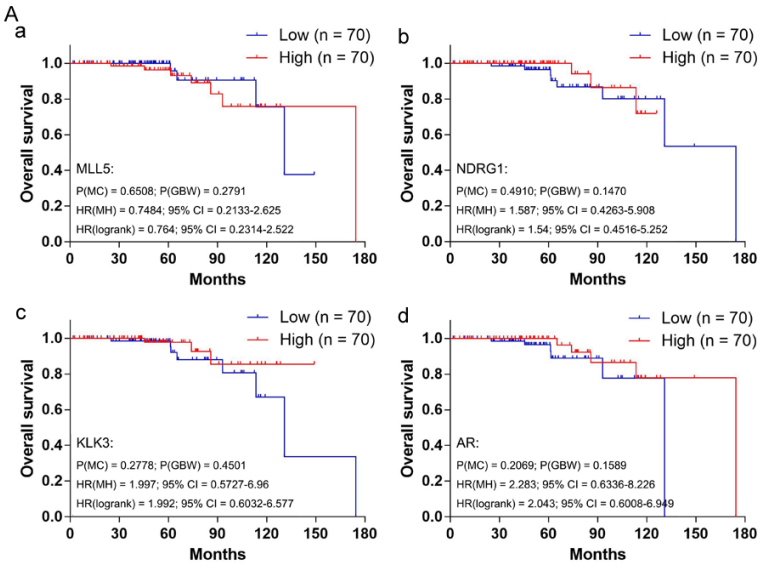

Supplementary Figure 2. No significant association was found between MLL5 expression and PCa patients' overall survival in the Taylor Prostate 3 database. A. Kaplan-Meier survival curves and Cox regression model for the association between the expression of MLL5 (a), NDRG1 (b), KLK3 (c), and AR (d) on patients' overall survival (with the median reported expression value as the cutoff; P (MC): *P* value from the log-rank (Mantel-Cox) test; P (GBW): *P* value from the Gehan-Breslow-Wilcoxon test; HR (MH): hazard ratio (Mantel-Haenszel); HR (log-rank): hazard ratio (log-rank); 95% CI: 95% confidence interval of the HR in the Low/High groups).